Synthesis of GABA$_A$ Receptor Agonists and Evaluation of their α-Subunit Selectivity and Orientation in the GABA Binding Site

Michaela Jansen,[†,‡,§,⊥] Holger Rabe,[‖,⊥] Axelle Strehle,[‖,§] Sandra Dieler,[†] Fabian Debus,[‖] Gerd Dannhardt,[†] Myles H. Akabas,[‡,*] and Hartmut Lüddens[‖,*]

Department of Medicinal Chemistry and Department of Psychiatry, Johannes Gutenberg-University, Mainz, Germany, and Departments of Physiology & Biophysics, Neuroscience and Medicine, Albert Einstein College of Medicine of Yeshiva University, Bronx, New York

Drugs used to treat various disorders target GABA$_A$ receptors. To develop α subunit selective compounds, we synthesized 5-(4-piperidyl)-3-isoxazolol (4-PIOL) derivatives. The 3-isoxazolol moiety was substituted by 1,3,5-oxadiazol-2-one, 1,3,5-oxadiazol-2-thione, and substituted 1,2,4-triazol-3-ol heterocycles with modifications to the basic piperidine substituent as well as substituents without basic nitrogen. Compounds were screened by [^{3}H]muscimol binding and in patch-clamp experiments with heterologously expressed GABA$_A$ α$_i$β$_3$γ$_2$ receptors (i = 1−6). The effects of 5-aminomethyl-3H-[1,3,4]oxadiazol-2-one **5d** were comparable to GABA for all α subunit isoforms. 5-piperidin-4-yl-3H-[1,3,4]oxadiazol-2-one **5a** and 5-piperidin-4-yl-3H-[1,3,4]oxadiazol-2-thione **6a** were weak agonists at α$_2$-, α$_3$-, and α$_5$-containing receptors. When coapplied with GABA, they were antagonistic in α$_2$-, α$_4$-, and α$_6$-containing receptors and potentiated α$_3$-containing receptors. **6a** protected GABA binding site cysteine-substitution mutants α$_1$F64C and α$_1$S68C from reacting with methanethiosulfonate-ethylsulfonate. **6a** specifically covalently modified the α$_1$R66C thiol, in the GABA binding site, through its oxadiazolethione sulfur. These results demonstrate the feasibility of synthesizing α subtype selective GABA mimetic drugs.

Introduction

γ-Aminobutyric acid type A receptors (GABA$_A$[a]) are responsible for most of the fast inhibitory synaptic transmission in mammalian brain. They belong to the Cys-loop receptor superfamily of ligand-gated ion channels. These receptors are formed by the pentameric assembly of homologous subunits and contain an anion-selective transmembrane channel. Numerous GABA$_A$ receptor subunits have been identified (α$_{1−6}$, β$_{1−3}$, γ$_{1−3}$, δ, π, ε, and θ), all of which are products of separate genes.[1–3] Most GABA$_A$ receptors contain two α, two β and either a γ or a δ subunit. Recombinant GABA$_A$ receptors with different subunit isoform composition display differing sensitivity to the endogenous agonist GABA.[4] The GABA$_A$ receptor subunits exhibit distinct, although overlapping, regional distribution patterns within the brain, with expression patterns changing during pre- to postnatal development.[5] In addition, in neurons expressing multiple receptor isoforms, subunit-selective targeting to distinct cellular domains has been observed.[6,7] The subunit isoform diversity and brain region specific expression patterns form the basis for the functional and pharmacological heterogeneity of GABAergic neurotransmission. Presently, most drug therapy for anxiety, epilepsy, and surgical sedation and often for insomnia targets GABA$_A$ receptor subtypes nonselectively, but the heterogeneity of the receptors theoretically holds the promise for brain region- or even cell-selective pharmacological intervention, which would increase the specificity of the effects and decrease the incidence of undesirable side effects.

Most of the known pharmacological heterogeneity of GABA$_A$ receptors concerns the sensitivity of the benzodiazepine site that is formed at the interface between the α and γ subunits.[8–10] Receptors lacking the γ$_2$ subunit or containing the α$_4$ or α$_6$ subunits are practically insensitive to benzodiazepine site agonists.[11–14] The two GABA binding sites are formed at the interfaces between the β and α subunits. Only a few different structural classes of ligands are known for the GABA binding site, reflecting the strict structural requirements for GABA$_A$ receptor recognition and activation. To date, these GABA binding site agonist compounds display little subunit subtype specificity with gaboxadol forming a class on its own as a "superagonistic" GABA mimetic.[15] A few compounds have been identified that neither bind to the benzodiazepine nor the GABA binding sites and yet still show subtype-selective antagonistic activity, these include furosemide, otherwise known as a Na$^+$/K$^+$/2Cl$^−$ cotransporter blocker, that selectively blocks α$_{(4/6)}$β$_{(2/3)}$γ$_2$ receptors,[16,17] and clozapine, an atypical antipsychotic drug that inhibits furosemide-insensitive α$_1$ containing receptors.[18]

Undesirable side effects, such as sedation and amnesia, often limit the clinical use of benzodiazepines[19] as well as the use of full agonists and of zero modulators of the GABA recognition site.[20] Different strategies exist to minimize undesirable effects: subtype-selective ligands or partial agonists. Studies with transgenic rodents have helped to dissect the α-subunit isoforms involved in specific pharmacologic effect of benzodiazepines. For example, α$_2$-containing receptors are primarily responsible for anxiolytic effects of benzodiazepines whereas α$_1$-containing receptors are more important for the sedative side effects.

* To whom correspondence should be addressed. For H.L.: Phone, +49 6131 175372; Fax, +49 6131 175590; E-mail: lueddens@uni-mainz.de. For M.H.A.: Phone, +1 718 430 3360; Fax, +1 718 430 8819; E-mail: makabas@aecom.yu.edu.

† Department of Medicinal Chemistry, University of Mainz.

‡ Departments of Physiology & Biophysics, Neuroscience and Medicine, Albert Einstein College of Medicine of Yeshiva University.

§ Present addresses: M.J., Department of Physiology and Biophysics, Albert Einstein College of Medicine of Yeshiva University; A.S., Université Louis Pasteur, Strasbourg, France.

‖ Department of Psychiatry, University of Mainz.

⊥ M.J. and H.R. contributed equally to this study.

[a] Abbreviations: ACh, acetylcholine; AChBP, acetylcholine binding protein; DTT, dithiothreitol; GABA, γ-aminobutyric acid; GABA$_A$, GABA type A receptors; MTS, methanethiosulfonate; MTSES$^−$, methanethiosulfonate ethylsulfonate; SCAM, substituted cysteine accessibility method.
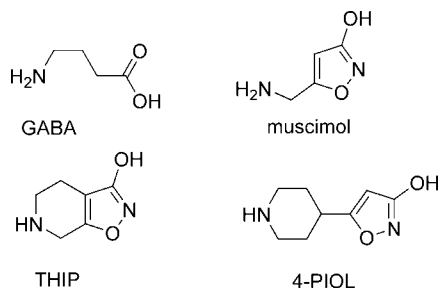
**Figure 1.** Structures of GABA, muscimol, THIP, and 4-PIOL.

Current research efforts focus on designing subunit-selective benzodiazepines.[21–27] In general, it seems desirable to have subtype-selective ligands that only act on a certain receptor subtype that is involved in transducing the desired effect and not on other subtypes that are involved in undesired effects. A complementary approach is to develop partial agonists of the GABA recognition site that induce only submaximal activation of specific α-subunit containing receptors. Under close to complete receptor occupancy, these partial agonists act as inhibitors of full agonists.[15] Partial agonists at the benzodiazepine site have also been investigated.[28–30]

In a previous study, we used binding studies on rat brain cryostat sections and patch-clamp experiments with heterologously expressed recombinant GABA$_A$ receptors to characterize the low-efficacy GABA mimetic 5-(4-piperidyl)isoxazol-3-ol (4-PIOL) (Figure 1) as a weak partial agonist or antagonist depending on the brain area and the GABA$_A$ receptor composition.[31,32] Therefore, we synthesized and functionally characterized different 5-(4-piperidyl)-1,3,4-oxadiazol- and 5-(4-piperidyl)-1,3,4-triazol-derivatives compounds structurally related to 4-PIOL.[33] The effects of other 4-PIOL derivatives on GABA$_A$ receptors have been studied previously.[34–40] All compounds were screened for efficacy and potency to GABA$_A$ receptors in native membranes using a [^{3}H]muscimol binding assay. Substances inducing changes in [^{3}H]muscimol binding in the micromolar concentration range were further analyzed in patch clamp recordings from GABA$_A$ receptors heterologously expressed in human embryonic kidney (HEK 293) cells. The α subunit specificity of these compounds was tested in α$_i$β$_3$γ$_2$ ($i = 1–6$) GABA$_A$ receptors by measuring the modulation of GABA-induced chloride current and the intrinsic activity of the compounds. We also sought to demonstrate that the actions of these new compounds were mediated through binding at the GABA-binding sites. We used a variant of the substituted cysteine accessibility method (SCAM) in order to identify the position and orientation of **6a** in the binding site.[41] Residues in the α subunit that line the GABA binding site have been identified based on the effects of mutations on electrophysiological properties,[42–44] photoaffinity labeling,[45] and SCAM.[46–48] They include those aligned with rat α$_1$ positions F64, R66, S68, and T129. Although crystal structures of GABA$_A$ receptor binding sites are not yet available, homology models based on the snail acetylcholine binding protein (AChBP) structure provide a reasonable molecular context in which to interpret our results.[49]

Synthesis

The synthetic procedures for the 5-(4-piperidyl)-1,3,4-oxadiazole- and 5-(4-piperidyl)-1,3,4-triazol-derivatives in this study are depicted in Schemes 1 and 2, whereas Schemes 3 and 4 depict specific variations of the 4-piperidyl moiety. Here we describe the synthesis of the 4-piperidyl-derivatives as an
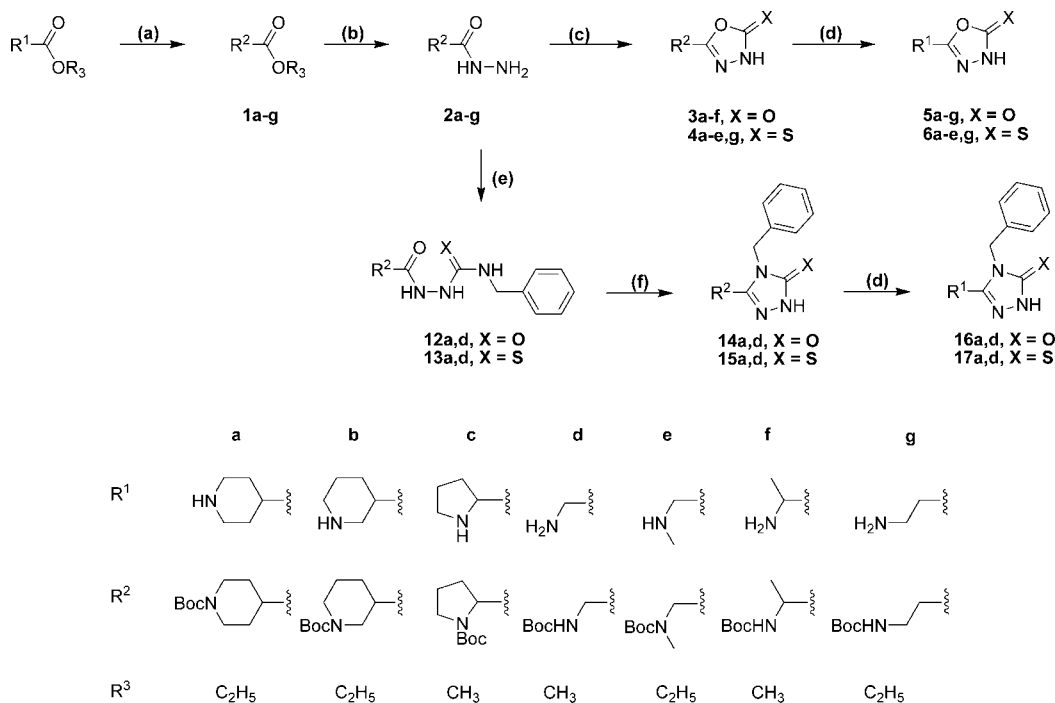
Scheme 1^a
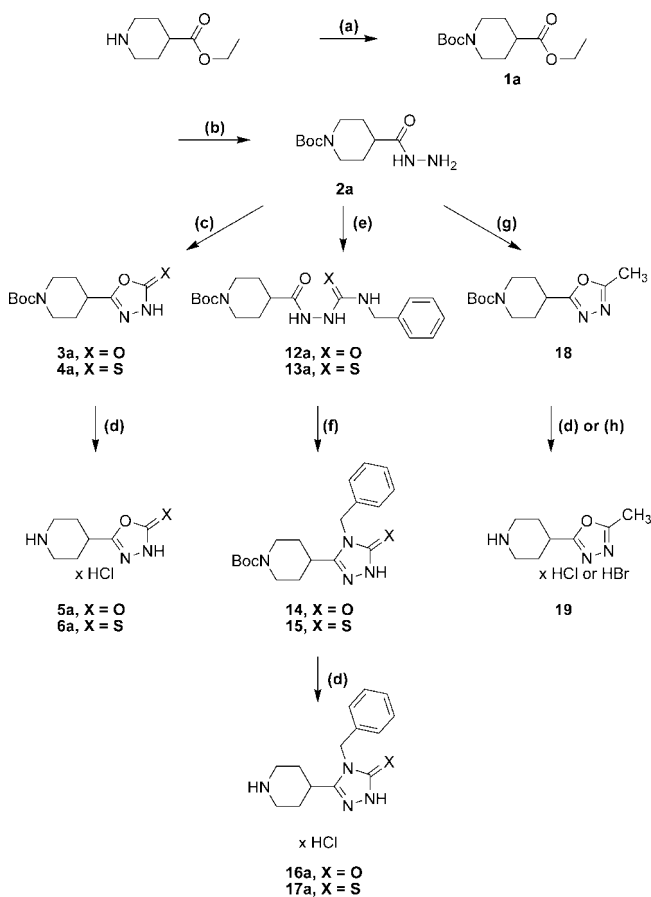
^{a} Reaction conditions: (a) Et$_3$N, Boc$_2$O in CH$_2$Cl$_2$ or NaHCO$_3$, Boc$_2$O in water; (b) NH$_2$NH$_2$; (c) CDI to obtain **3**; CS$_2$ to obtain **4**; (d) 2.3 N ethanolic HCl; (e) PhCH$_2$NCX; (f) 2% NaOH; (g) H$_3$CC(OC$_2$H$_5$)$_3$; (h) HBr/HAc.
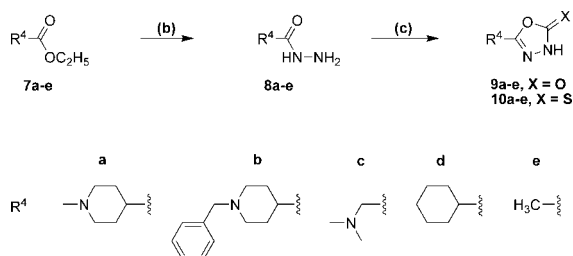
Scheme 2^a
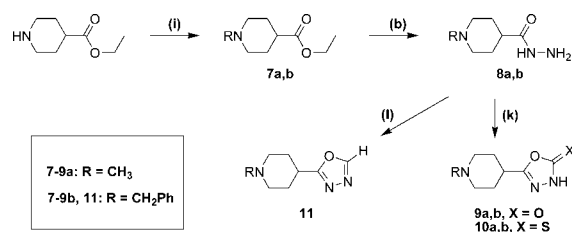
^{a} Reaction conditions: (b) NH$_2$NH$_2$; (i) CH$_2$O, HCOOH to obtain **7a**; PhCH$_2$Cl to obtain **7b**; (k) triphosgene to obtain **9a,b**; CS$_2$ to obtain **10a,b**; (l) HC(OC$_2$H$_5$)$_3$.

example. The secondary amine function of 4-piperidine-carboxylic acid ester was either protected with the *t*-butoxycarbonyl (Boc) group using di-*t*-butyldicarbonate and NaHCO$_3$ in water or triethylamine in methylene chloride (Scheme 1: **1a**) or alkylated using formaldehyde, formic acid, or benzylchloride (Scheme 2: **7a,b**). Subsequently, the esters were converted to the corresponding acid hydrazides (Scheme 1: **2a;** Scheme 2: **8a,b**) by refluxing the ester in an excess of hydrazine hydrate. The 1,3,4-oxadiazol-2-ones (Scheme 1: **3a;** Scheme 2: **9a,b**) were prepared by refluxing the hydrazides with *N,N'*-carbonyldiimidazol (CDI) in the presence of triethylamine in a mixture of THF and DMF. The corresponding 1,3,4-oxadiazol-2-thiones (Scheme 1: **4a;** Scheme 2: **10a,b**) were synthesized by refluxing the hydrazides with carbonyldisulfide in an ethanolic potassium hydroxide solution. Theoretically, oxadiazol-2-ones and -thiones can exist in two tautomeric forms, the amide form and the imino-

Scheme 3[a]

[a] Reaction conditions as given in Schemes 1 and 2.

Scheme 4[a]

[a] Reaction conditions as given in Schemes 1 and 2.

alcohol form. IR, UV, and NMR spectra, however, indicate that they exist predominantly in their amide-form.[50] The hydrazide **2a** was also cyclized with triethoxyethane to yield the 2-methyl-1,3,4-oxadiazol-derivative (Scheme 1: **18**). Reaction of the hydrazide **2a** with benzylisocyanate or benzylisothiocyanate produced the acylated semicarbazide derivatives **12a** and **13a**, which were converted to benzyl-1,3,4-oxadiazoles **14** and **15** by refluxing with NaOH in an aqueous solution (Scheme 1). *N*-methyl-piperidin-4-yl carboxylic acid hydrazide (**8b**) was reacted with triethoxymethane to yield the 2-unsubstituted 1,3,4-oxadiazol-derivative **11** (Scheme 2). The 4-piperidyl moiety was varied as outlined in Scheme 3 and 4. It was substituted by a 3-piperidyl and a 2-pyrrolidinyl moiety, or residues that lead to derivatives that mimic glycine, sarcosine, alanine, and β-alanine (Scheme 3) as well as *N*-alkylated 4-piperidinyl-compounds, dimethylglycine, and two compounds without an amine function (Scheme 4). The last step during the synthesis of compounds **5a–g**, **6a–e,g**, **16a**, **17a**, and **19** was the removal of the Boc-protective group with hydrogen chloride (Scheme 1 and 3).
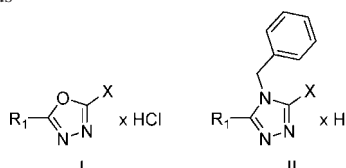
Pharmacology

[³H]Muscimol Binding. Compounds were initially screened by probing their ability to compete with [³H]muscimol binding to the GABA recognition site in native cortical and cerebellar

membranes. We used two concentrations (100 μM and 1 mM) of the compounds. This approach allowed us to eliminate compounds with very low binding affinity. Additionally, we compared the binding of [³H]muscimol to membranes from two brain structures: cortex, containing $α_1$-$α_5$ receptors, and cerebellum, enriched in $α_1$- and the exclusive source of $α_6$-containing GABA$_A$ receptors (Table 1), to enable us to detect pronounced differences in subtype selectivity of the compounds.

Of the 28 compounds tested, six fulfilled our criteria for full binding analysis in that, at 100 μM, they inhibited muscimol binding by at least 30% (Table 1). These six included **5a**, **5d**, **5g**, **6a**, **6d**, and **19**. For these compounds, we determined the IC$_{50}$ values for inhibition of [³H]muscimol binding to cortical and cerebellar membranes (Table 2, Figure 2). **5d** showed the highest affinity with an IC$_{50}$ of 1.4 μM, and **5a** exhibited the lowest affinity, 183 μM (Table 2). None of the six compounds displayed significant differences between IC$_{50}$ determined in cortical vs cerebellar membranes, although compound **5g** showed a significant difference between the pseudo-Hill coefficient determined in cortical vs cerebellar membranes, 0.63 vs 0.92, respectively, whereas no difference in any measure was detected for the other compounds (Table 2).

HEK293 Electrophysiology. We characterized the functional effects of four compounds on $α_iβ_3γ_2$ ($i = 1-6$) GABA$_A$ receptors using patch-clamp experiments with heterologously expressed GABA$_A$ receptors. This allowed us to determine directly the GABA$_A$ receptor α subunit specificity for these four compounds identified as the most potent inhibitors in the [³H]muscimol binding assays described above. Transiently transfected HEK 293 cells coexpressing an α variant plus $β_3$ and $γ_2$S and enhanced green fluorescent protein (EGFP) were used in these experiments. EGFP fluorescence facilitated the identification of transfected cells for patch clamping. For each compound, we applied a series of increasing drug concentrations either alone, to assess the intrinsic agonist activity, or together with the approximate EC$_{20}$ to EC$_{25}$ concentration of GABA, to

Table 1. Percent Inhibition of [^{3}H]Muscimol Binding to Well-Washed Membranes from Rat Cortex and Cerebellum by 100 μM and 1 mM of Test Compounds[a]

#	R	X	cortex		cerebellum	
			100 μM	1 mM	100 μM	1 mM
5a	HN—⬡—	OH	38 ± 15 (4)	79 ± 7 (4)	38 ± 20 (4)	77 ± 11 (4)
5b	HN—⬠—	OH	1 ± 11 (3)	24 ± 5 (4)	9 ± 9 (4)	10 ± 7 (4)
5c	(pyrrolidine)	OH	5 ± 7 (3)	10 ± 3 (3)	8 ± 1 (3)	13 ± 4 (3)
5d	H$_2$N—	OH	99 ± 4 (3)	104 ± 2 (3)	97 ± 6 (3)	102 ± 6 (3)
5e	HN—	OH	14 ± 3 (3)	58 ± 4 (3)	22 ± 3 (3)	64 ± 1 (3)
5f	H$_2$N—	OH	26 ± 25 (3)	16 ± 4 (3)	13 ± 17 (3)	34 ± 4 (3)
5g	H$_2$N—	OH	85 ± 5 (3)	100 ± 1 (3)	89 ± 1 (3)	98 ± 0 (3)
6a	HN—⬡—	SH	68 ± 5 (4)	94 ± 2 (4)	64 ± 9 (4)	91 ± 2 (4)
6b	HN—⬠—	SH	12 ± 17 (4)	51 ± 9 (4)	15 ± 3 (4)	42 ± 5 (4)
6c	(pyrrolidine)	SH	21 ± 19 (3)	36 ± 6 (3)	-2 ± 0 (3)	31 ± 4 (3)
6d	H$_2$N—	SH	58 ± 14 (3)	99 ± 9 (3)	61 ± 1 (3)	95 ± 2 (3)
6e	HN—	SH	17 ± 1 (3)	24 ± 9 (3)	9 ± 9 (3)	16 ± 4 (3)
6g	H$_2$N—	SH	9 ± 7 (3)	61 ± 6 (3)	23 ± 5 (3)	67 ± 1 (3)
9a	N—⬡—	OH	4 ± 7 (4)	27 ± 5 (4)	6 ± 5 (4)	26 ± 6 (4)
9b	(N-benzyl piperidine)	OH	12 ± 6 (4)	50 ± 3 (4)	7 ± 4 (4)	30 ± 8 (4)
9c	N—	OH	3 ± 1 (3)	27 ± 5 (3)	5 ± 5 (3)	26 ± 3 (3)
9d	⬡—	OH	18 ± 1 (3)	-2 ± 7 (3)	-11 ± 11 (3)	1 ± 12 (3)
9e	H$_3$C—	OH	7 ± 11 (3)	26 ± 3 (3)	3 ± 4 (3)	4 ± 7 (3)
10a	N—⬡—	SH	6 ± 6 (4)	48 ± 6 (4)	8 ± 10 (4)	27 ± 8 (4)
10b	(N-benzyl piperidine)	SH	3 ± 13 (4)	33 ± 14 (4)	6 ± 2 (4)	30 ± 5 (4)
10c	N—	SH	22 ± 8 (3)	47 ± 7 (3)	3 ± 8 (3)	37 ± 6 (3)
10d	⬡—	SH	10 ± 1 (3)	18 ± 2 (3)	0 ± 8 (3)	-3 ± 3 (3)
10e	H$_3$C—	SH	20 ± 4 (3)	10 ± 1 (3)	-4 ± 4 (3)	-3 ± 10 (3)
11	(N-benzyl piperidine)	H	-5 ± 3 (3)	1 ± 1 (3)	1 ± 3 (3)	-5 ± 4 (3)
16a (II)	HN—⬡—	OH	18 ± 3 (3)	56 ± 3 (3)	14 ± 1 (3)	52 ± 2 (3)
16d (II)	H$_2$N—	OH	4 ± 3 (3)	11 ± 1 (3)	1 ± 4 (3)	2 ± 4 (3)
17a (II)	HN—⬡—	SH	-6 ± 11 (3)	-	13 ± 18 (3)	-
17d (II)	H$_2$N—	SH	*	*	*	*
19	HN—⬡—	-CH$_3$	48 ± 8 (3)	87 ± 5 (3)	56 ± 5 (3)	91 ± 1 (3)

[a] Given are the means ± SD with the number of experiments in brackets. Compound **17a** was insoluble at 1 mM and therefore not tested at this concentration. Structure I applies except where II is specifically indicated. Compounds for which an IC$_{50}$ is reported in Table 2 are shaded grey. *: inactive.

determine its GABA-modifying activity. The GABA EC$_{20-25}$ concentrations used for the different α subunits are shown in Table 3.
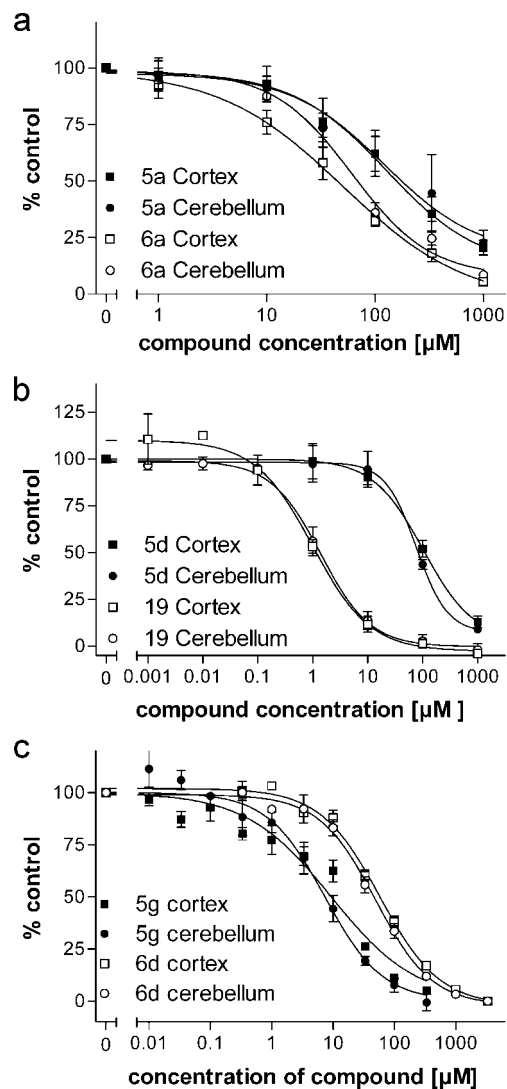
Figure 2. Dose−response curves as measured against [^{3}H]muscimol binding to cortical (squares) and cerebellar (circles) membranes. Binding data were normalized to the binding in the absence of any inhibitor set to 100%. Error bars indicate the SEM for at least three independent tissue preparations.

Intrinsic Agonist Activity (5a). (5-Piperidin-4-yl-3*H*-[1,3,4]oxadiazol-2-one hydrochloride) and **6a** (5-piperidin-4-yl-3*H*-[1,3,4]oxadiazol-2-thione hydrochloride) showed limited intrinsic activity in α_1, α_4, and α_6 containing receptors (Figure 3). At 1 mM, the induced currents were less than 10% of the currents induced by the approximate EC$_{100}$ GABA concentrations (Figure 4). In contrast, on α_2, α_3, and α_5 containing receptors, 1 mM **5a** caused currents of 17 ± 1%, 18 ± 2%, and 34 ± 3% of the maximal GABA-induced currents. On the same receptors, 1 mM **6a** induced currents that were 23 ± 5%, 13 ± 2%, and 48 ± 4% of the maximal GABA-induced currents.

5d (5-aminomethyl-3*H*-[1,3,4]oxadiazol-2-one hydrochloride) induced desensitizing currents in all GABA$_A$ receptor combinations tested in a dose-dependent manner with an efficacy >50% of the maximal GABA-induced currents and an α subunit specific potency (Table 4, Figure 3). Receptors containing α_6 subunits were most sensitive, with an EC$_{50}$ of 30 μM and receptors containing the α_3 subunit were the least sensitive with a **5d** EC$_{50}$ of ca. 2300 μM.

The ability of **19** (4-(5-methyl-[1,3,4]oxadiazol-2-yl)-piperidine hydrochloride) to directly activate GABA$_A$ receptors was restricted to α_6 containing receptors, where it induced currents

Table 2. Binding Parameters of Selected Compounds against 6 nM [^{3}H]Muscimol in Crude Membrane Preparations of Rat Cortex and Cerebellum Determined by Nonlinear Regression[a]

	cortex				cerebellum			
	log IC$_{50}$	IC$_{50}$ [μM]	η	n	log IC$_{50}$	IC$_{50}$ [μM]	η	n
5a	2.262 ± 0.185	183	0.86 ± 0.10	4	2.089 ± 0.170	123	0.79 ± 0.06	3
5d	0.139 ± 0.119	1.4	1.12 ± 0.13	3	0.048 ± 0.082	1.1	0.90 ± 0.21	3
5g	0.971 ± 0.074	9.4	0.63 ± 0.06	4	0.868 ± 0.065	7.4	0.92 ± 0.11	3
6a	1.668 ± 0.153	47	0.99 ± 0.09	3	1.819 ± 0.048	66	1.03 ± 0.08	4
6d	1.758 ± 0.074	57	0.92 ± 0.05	3	1.690 ± 0.081	49	0.96 ± 0.12	4
19	2.039 ± 0.067	109	0.88 ± 0.08	3	1.879 ± 0.081	76	0.91 ± 0.05	3

[a] Given are the means ± SEM of the decadic logarithm of the IC$_{50}$ in μM, the corresponding pseudo-Hill coefficient η, and the number of experiments n.

Table 3. GABA Concentrations and the Corresponding Relative Effective Concentration that Induces a Response around the EC$_{20}$ When Applied to GABA$_A$ Receptors $\alpha_i\beta_3\gamma_2$ ($i = 1-6$) Transiently Expressed in HEK 293 Cells[a]

α subunit	GABA [μM]	EC
α_1	2.0	25 ± 2.3
α_2	4.0	24 ± 1.9
α_3	8.0	22 ± 2.1
α_4	5.0	25 ± 2.0
α_5	3.0	22 ± 2.1
α_6	0.5	20 ± 2.2

[a] Given are the mean ± SEM.

$29 \pm 4\%$ of the maximal GABA-evoked currents. With all of the other α subunits 1 mM **19** induced a current less than 10% of the maximal GABA-induced current.

GABA Modulatory Effect. 5a showed a slight dose-dependent potentiating effect on α_3 and α_5 containing GABA$_A$ receptors with maximal current potentiation by 1 mM **5a** of $22 \pm 11\%$ for α_3 and $34 \pm 5\%$ for α_5 containing receptors (Figure 4). In all other α subunits, its action was antagonistic on GABA-induced currents with similar potency. Its antagonistic efficacy was highest in α_1 containing receptors, where 1 mM **5a** inhibited GABA-induced current by $77 \pm 3\%$. At this concentration, **5a** inhibited GABA-induced currents of other α subunits by $42 \pm 2\%$ for α_2, $52 \pm 5\%$ for α_4, and $41 \pm 4\%$ for α_6.

6a (5-piperidin-4-yl-3H-[1,3,4]oxadiazol-2-thione hydrochloride), the thioderivative of **5a**, had similar effects to **5a** except on α_2 containing receptors. **6a** potentiated GABA-induced currents in $\alpha_5\beta_3\gamma_2$ receptors to an extent similar to that described for **5a**, but on $\alpha_3\beta_3\gamma_2$ receptors, the potentiating effect of **6a** was higher with a current potentiation of $114 \pm 8\%$ at 1 mM. In contrast to **5a**, in α_2-containing receptors, low concentrations of **6a** potentiated submaximal GABA-induced currents with maximal potentiation of $39 \pm 4\%$ at 1 μM, whereas at 1 mM, **6a** inhibited GABA currents by $24 \pm 9\%$. **6a** also inhibited GABA-induced currents in α_1, α_4, and α_6 containing receptors.

5d (5-aminomethyl-3H-[1,3,4]oxadiazol-2-one hydrochloride) potentiated the GABA-induced currents for all of the α subunit isoforms with similar potency, apparent EC$_{50}$ values ranged between 100 and 300 μM (Figure 3). The efficacy was similar in α_1, α_2, α_3, and α_4 containing receptors with current potentiation of $302 \pm 35\%$, $324 \pm 40\%$, $311 \pm 18\%$, and $334 \pm 13\%$ at 1 mM, respectively. The **5d** efficacy was significantly enhanced in receptors comprising α_5 ($423 \pm 25\%$) and α_6 ($437 \pm 21\%$) subunits with p of <0.01 in a two-sided t test compared to α_1 containing receptors.

Lastly, we analyzed the GABA$_A$ receptor α subunit specificity of **19** (4-(5-methyl-[1,3,4]oxadiazol-2-yl)-piperidine hydrochloride) and its hydrobromide with electrophysiological methods. This novel compound increased the GABA-induced currents in all GABA$_A$ receptor combinations tested with similar potency. The efficacy shows a slight subtype specificity that could be

divided into two significantly different groups with p of <0.01 in a two-sided t test. The group with higher efficacy consisting of α_2, α_4, α_5, and α_6 with positive modulation of the GABA-induced currents ranging from 48% in α_2 to 87% in α_6 at 1 mM **19**. The positive modulation efficacy was smaller for α_3 and α_1 containing receptors, where compound **19** potentiated the GABA-induced currents by $11\% \pm 2$ and by $21\% \pm 5$, respectively.

Two-Electrode Voltage Clamp Electrophysiology in *Xenopus laevis* Oocytes

On the basis of the diverse set of effects, potentiation, inhibition, and direct activation seen with the compounds, we sought to demonstrate that they bound in the GABA binding site. These experiments focused on compound **6a**. We used a series of cysteine-substitution mutants in the GABA binding site.

Determination of GABA EC$_{50}$ Values. GABA dose−response relationships were determined for wild type and mutant $\alpha_1\beta_2$ receptors expressed in *Xenopus* oocytes (Table 5). Mutant α_1S68Cβ_2 receptors had an EC$_{50}$ value comparable to $\alpha_1\beta_2$ wt receptors. In contrast, the EC$_{50}$ values for the mutants α_1T129Cβ_2, α_1F64Cβ_2, and α_1R66Cβ_2 were increased 14-fold, 43-fold, and 554-fold, respectively, compared to wild type, in agreement with previously published data.[46,47]

Determination of 6a EC$_{50}$. **6a** acted as an agonist on $\alpha_1\beta_2$ wt, α_1F64Cβ_2, and α_1S68Cβ_2 receptors. To prove that the **6a**-induced currents were mediated by GABA$_A$ receptor activation, we tested the ability of picrotoxinin, an open channel blocker, to inhibit the **6a** induced currents. Coapplication of 100 μM picrotoxinin and 10 mM **6a** inhibited **6a**-induced currents by 80−90% (Figure 5). We infer that **6a** directly activates GABA$_A$ receptors.

We determined the **6a** EC$_{50}$ for the Cys-substitution mutant receptors (Table 5). For wt receptors, the **6a** EC$_{50}$ was 9.5 mM. It was similar for α_1S68Cβ_2. For α_1F64Cβ_2, the **6a** EC$_{50}$ was 0.6 fold less than for wt.

The efficacy of **6a** as compared to GABA was significantly greater for α_1F64Cβ_2 receptors compared to $\alpha_1\beta_2$ wt and α_1S68Cβ_2. A 30 mM concentration of **6a** produced currents that were 60, 20, and 17% as large as the maximal GABA current for α_1F64Cβ_2, $\alpha_1\beta_2$ wt, and α_1S68Cβ_2 receptors, respectively. Higher concentrations of **6a** were not used due to the limited supply of the compound. The Hill coefficient of the **6a** dose−response relationship was increased compared to GABA.

Determination of 6a IC$_{50}$ Values of the Mutants. Coapplication of **6a** and GABA inhibited the GABA-induced currents. We performed competition experiments to determine the **6a** IC$_{50}$ for inhibiting GABA EC$_{20}$ currents with $\alpha_1\beta_2$ wt, α_1F64Cβ_2, and α_1S68Cβ_2 receptors (Table 5). One mM **6a** inhibited the EC$_{20}$ GABA current by more than 90% in these
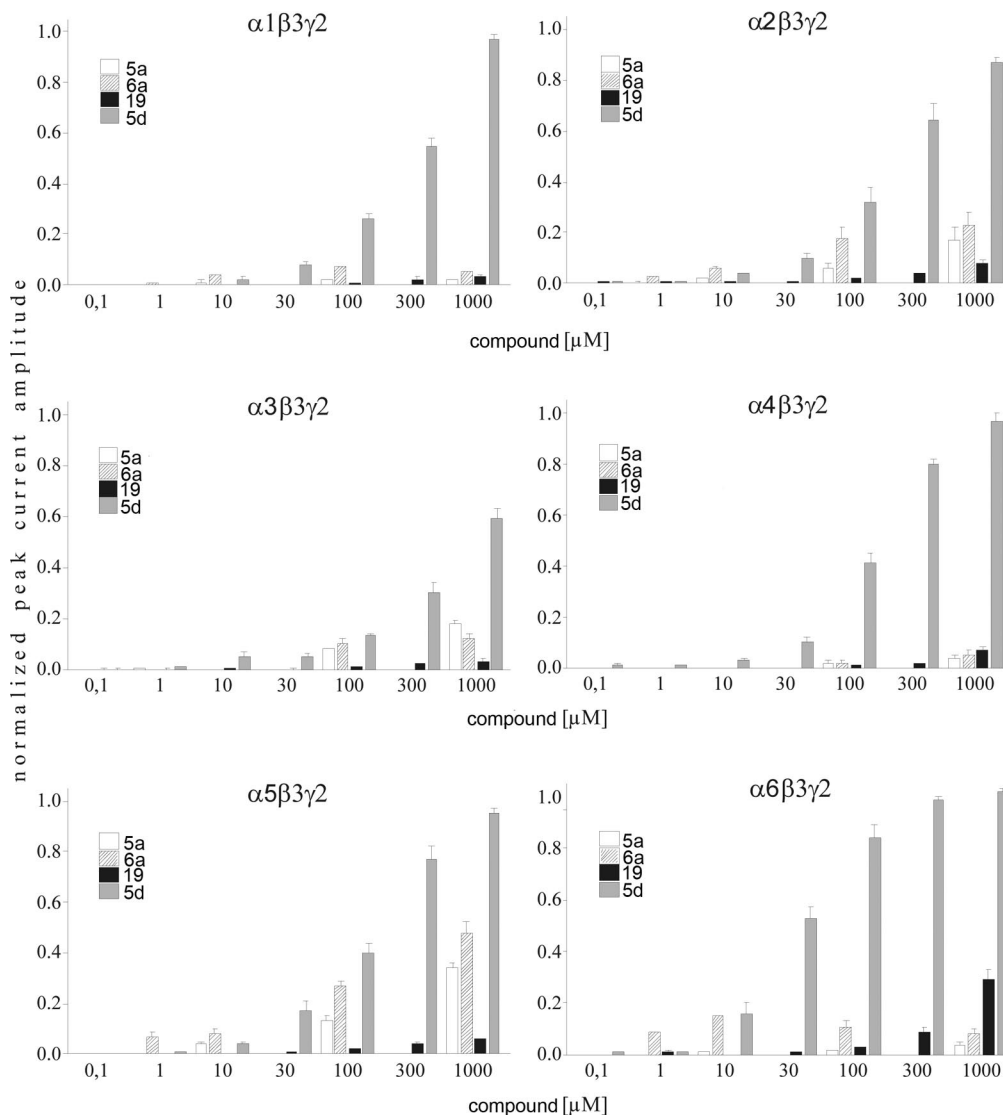
Figure 3. Whole-cell recordings of HEK 293 cells expressing recombinant rat $\alpha_i\beta_3\gamma_2$ ($i = 1-6$) GABAA receptors. Currents were normalized to the maximally GABA-induced current at the approximate EC_{100}. To test the intrinsic activity, different concentrations of the 5-(4-piperidyl)-1,3,4-oxadiazol-derivates tested were applied to the cells. Error bars indicate the SEM for at least four cells.

receptors. The residual GABA currents observed during the coapplication of 1 mM **6a** and GABA EC_{20} concentration, were $6.8 \pm 1.0\%$ ($n = 4$) for $\alpha_1\beta_2$ wt, $9.0 \pm 2.0\%$ ($n = 3$) for $\alpha_1F64C\beta_2$, and $3.0 \pm 1.8\%$ ($n = 6$) for $\alpha_1S68C\beta_2$. Because the **6a**-GABA competition experiments were done at a relatively low GABA concentration, we decided that for the protection experiments the **6a** concentration should be at least 1 mM.

Effects of MTS-Reagents on the Cysteine Mutants and Reaction Rates. Methanethiosulfonate (MTS) reagents react 10^9 times faster with ionized thiolates (S^-) than with thiols (SH);[51] thus, they are much more likely to react with water-accessible cysteine, which can ionize. We monitored the MTS reaction with a substituted cysteine by its effect on the channel's macroscopic currents.

Application of the anionic reagent MTS-ethylsulfonate (MTSES$^-$) did not affect the GABA current in $\alpha_1\beta_2$ wt receptors (data not shown).[46] After complete reaction with MTSES$^-$ and/ or MTSEA-biotin, subsequent GABA EC_{50} currents were inhibited to a similar extent for $\alpha_1F64C\beta_2$, $\alpha_1R66C\beta_2$, $\alpha_1S68C\beta_2$, and $\alpha_1T129C\beta_2$ receptors (see Table 6). We infer that in the cysteine-substitution mutants, changes in the GABA-induced current after MTS application were due to the covalent modification of the engineered cysteine.

The observed second-order rate constants for reaction with MTSES$^-$ were 11300 ± 700 M^{-1}/s for $\alpha_1F64C\beta_2$, 48 ± 7 M^{-1}/s for $\alpha_1R66C\beta_2$, and 240 ± 40 M^{-1}/s for $\alpha_1S68C\beta_2$, which are in agreement with previously reported results (Table 7, Figure 6).[46] For $\alpha_1R66C\beta_2$ and $\alpha_1T129C\beta_2$, the second-order reaction rate constant for MTSEA-biotin with $\alpha_1R66C\beta_2$ was 5500 ± 1600 M^{-1}/s and with $\alpha_1T129C\beta_2$ was 6700000 ± 1100000 M^{-1}/s (Table 6). All reaction rates were well fit by a monoexponential function. For each mutant receptor, however, there are two engineered cysteine residues because $\alpha\beta$-receptors are pentameric and their subunit stoichiometry is proposed to be $2\alpha:3\beta$.[52,53] Either the two cysteine residues from each receptor reacted at the same rate, or reaction at only one residue gave the complete effect. These two possibilities are indistinguishable with the present methods.

Protection of Cysteine Mutants by GABA and 6a. If an engineered cysteine forms part of a ligand-binding site, then the presence of the ligand in the binding site should reduce the ability of MTS reagents to react with the cysteine. This should decrease the measured MTS reaction rate in the presence of the ligand. It was reported previously that in the presence of GABA, α_1F64C, α_1R66C, and α_1S68C are protected from reaction with MTS reagents (MTSEA-biotin, MTSES$^-$, MTSEA$^+$).[46,47] This protec-
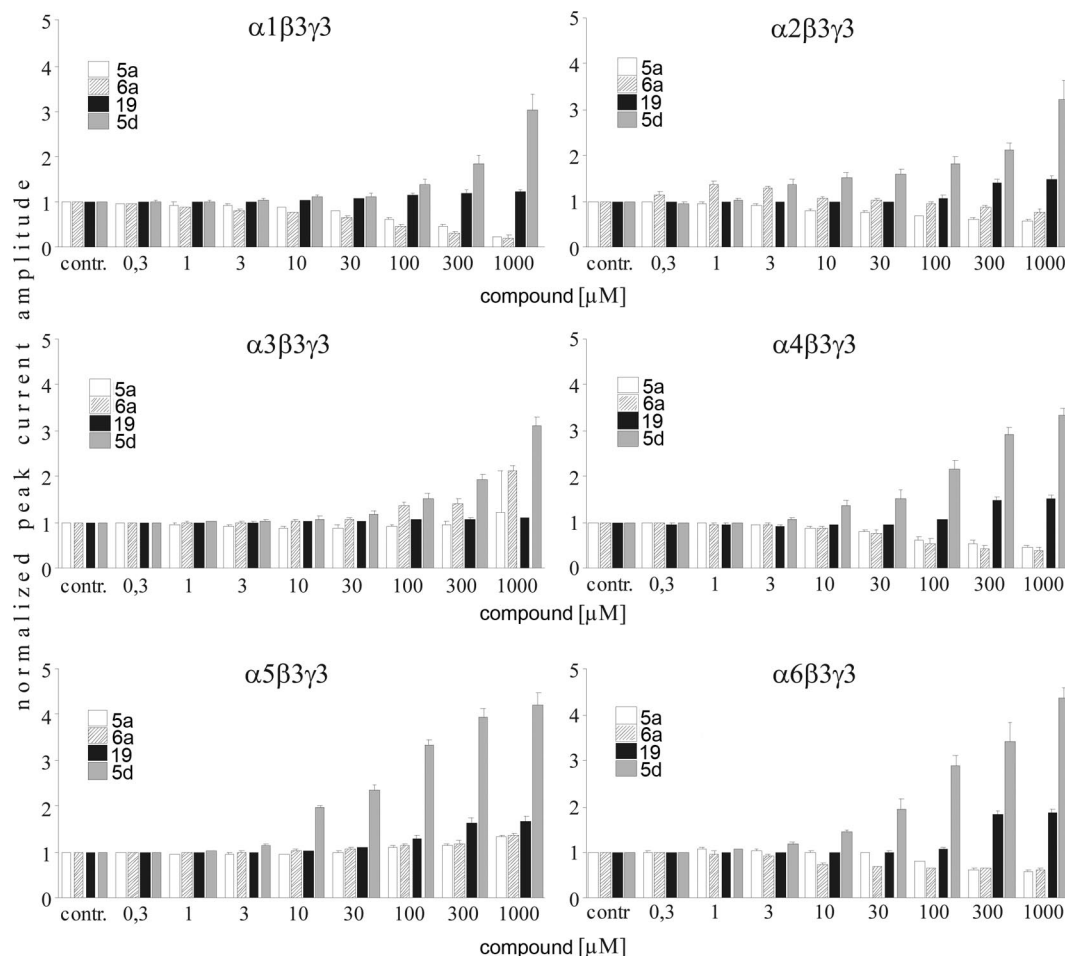
Figure 4. Whole-cell recordings of HEK 293 cells expressing recombinant rat $\alpha_i\beta_3\gamma_2$ ($i = 1-6$) GABA$_A$ receptors. Currents were normalized to the GABA concentrations specific for the receptor subtype under in vitro conditions. Different concentrations of the 5-(4-piperidyl)-1,3,4-oxadiazol-derivates tested were coapplied with GABA concentrations around the EC$_{20}$. Error bars indicate the SEM for at least four cells.

Table 4. Maximal Intrinsic Activity of 1 mM **5d** Normalized to the Approximate Maximal GABA-Induced Current ($I/I_{maxGABA}$) and the **5d** EC$_{50}$ and Hill Coefficient on $\alpha_i\beta_3\gamma_2$ ($i = 1-6$) GABA$_A$ Receptors[a]

α subunit	$I/I_{maxGABA}$	EC$_{50}$ [μM]	Hill
α_1	0.93 ± 0.03	280 ± 17	0.99 ± 0.05
α_2	0.88 ± 0.02	182^b	1.23^b
α_3	0.59 ± 0.04	2300^b	0.81^b
α_4	0.97 ± 0.01	128 ± 8	1.56 ± 0.11
α_5	0.95 ± 0.03	137 ± 14	1.31 ± 0.12
α_6	1.03 ± 0.01	30 ± 3	1.41 ± 0.14

[a] Data are means $\pm$ SEM. [b] Values of an extrapolated dose−response curve.

Table 5. Summary of Dose−Response Data and **6a** Competition Data Using a GABA EC$_{20}$ Concentration from Cysteine-Substituted and wt $\alpha_1\beta_2$ GABA$_A$ Receptors

	GABA			6a			
receptor	EC$_{50}$ (μM)	mutant/wt	n	EC$_{50}$ (mM)	n	IC$_{50}$ (μM)	n
$\alpha_1\beta_2$ wt	10.0 ± 1.2	1	6	9.5 ± 0.02	2	59 ± 6	4
α_1F64C β_2	430 ± 40	43	6	5.5 ± 0.2	4	56 ± 12	3
α_1R66C β_2	5540 ± 210	554	6	n.d.		n.d.	
α_1S68C β_2	6.5 ± 0.5	0.65	5	10.0 ± 0.3	2	46 ± 5	3
α_1T129C β_2	136 ± 6	13.6	6	n.d.		n.d.	

tion may be due either to direct steric protection due to the presence of GABA in the binding site or to a GABA-induced conformational change reducing the accessibility of these residues to the MTS reagent. The fact that these cysteine mutants were also protected
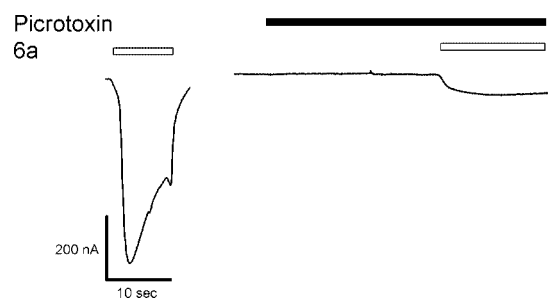

Figure 5. Picrotoxinin blocks **6a** induced currents in $\alpha_1\beta_2$ wt receptors. The first trace shows a **6a** induced current. The second trace was recorded during a 20 s application of picrotoxinin, immediately followed by a coapplication of **6a** and picrotoxinin.

Table 6. Extent of Inhibition of GABA-Induced Currents after Reaction with MTS Reagent[a]

	α_1F64C	α_1R66C	α_1S68C	α_1T129C
MTSES$^-$	89 ± 3 (4)	62 ± 3 (4)	60 ± 10 (3)	n.d.
MTSEA-biotin	n.d.	75 ± 4 (9)	n.d.	60 ± 3 (6)

[a] Inhibition (% $\pm$ SEM (n)) for GABA EC$_{50}$ currents after complete reaction with MTSES$^-$ and MTSEA-biotin on GABA$_A$ receptors containing the cited cys-engineered α_1 subunit together with the β_2 subunit expressed in Xenopus oocytes. n.d. = not determined.

from modification by SR-95531, a competitive antagonist, implies that the mechanism of protection is a steric not an allosteric one.[46,47]

α_1F64Cβ_2 and α_1S68Cβ_2 receptors were protected from reaction with MTSES$^-$ by both GABA and **6a** (Figures 7 and

Table 7. MTS-Reagent Reaction Rates

receptor	MTS-reagent	reaction rate [M^{-1}/s]	n
α_1F64C β_2	MTSES$^-$	11300 ± 700	3
α_1R66C β_2	MTSES$^-$	48 ± 7	5
	MTSEA-biotin	5500 ± 1600	6
α_1S68C β_2	MTSES$^-$	240 ± 40	4
α_1T129C β_2	MTSEA-biotin	6700000 ± 1100000	3

8). In control experiments with α_1F64Cβ_2, a 12 s application of 10 μM MTSES$^-$ caused an 87 ± 3% (n = 4) reduction in subsequent GABA EC$_{50}$ test currents (Figure 7A). In contrast, a 12 s coapplication of 10 μM MTSES$^-$ with 3.6 mM GABA caused only a 35 ± 1% (n = 5) reduction of the subsequent GABA-induced currents (Figure 7B) and coapplication of 10 μM MTSES$^-$ with 10 mM **6a** resulted in only a 47 ± 6% (n = 4) reduction (Figure 7C) of the subsequent GABA-induced currents. Thus, the extent to which MTSES$^-$ could react with α_1F64Cβ_2 was reduced by the presence of GABA and **6a**. This implies that both agonists protected the engineered cysteine from covalent modification.

Similarly, for the α_1S68Cβ_2 mutant, application of 450 μM MTSES$^-$ for 12 s reduced the subsequent GABA test currents by 77 ± 5% (n = 4) (Figure 8). Coapplication of 450 μM MTSES$^-$ with 65 μM GABA or 10 mM **6a** only reduced the subsequent GABA test currents by 40 ± 2% (n = 4) and 10 ± 4% (n = 4), respectively, consistent with protection of the α_1S68C cysteine residue.

In similar experiments with α_1R66Cβ_2 receptors, 10 mM **6a** demonstrated slight, but significant protection of the engineered cysteine from reaction with MTSES$^-$ (Figure 8). A 12 s application of 2 mM MTSES$^-$ to α_1R66Cβ_2 inhibited 91 ± 3% (n = 6) of the subsequent GABA EC$_{50}$ current. Coapplication of 35 mM GABA with MTSES$^-$ inhibited 49 ± 6% (n = 3) of the subsequent test currents, consistent with protection by GABA. In contrast, application of 10 mM **6a** with 2 mM MTSES$^-$ resulted in 77 ± 4% (n = 5) inhibition of the subsequent GABA test currents. Comparable results were obtained for MTSEA-biotin, application of 30 mM **6a** with
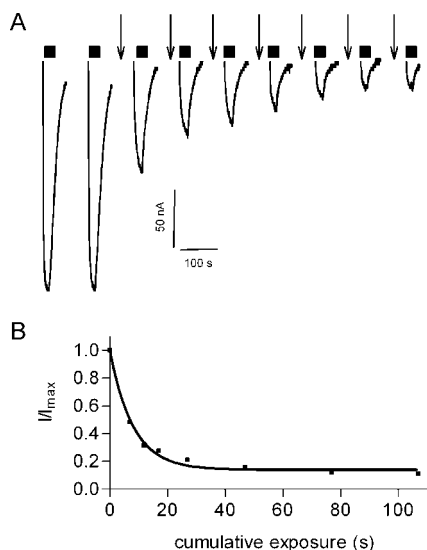
Figure 6. MTSES$^-$ reaction rate with the α_1F64Cβ_2 cysteine mutant. (A) EC$_{50}$ GABA current traces were recorded initially and after each brief application of 10 μM MTSES$^-$ (↓). Currents during MTSES$^-$ application (↓) are not shown. (B) GABA test currents were normalized to the initial GABA current (I_{max}) and plotted versus cumulative MTSES$^-$ exposure time. Data were fit to a monoexponential decay function.
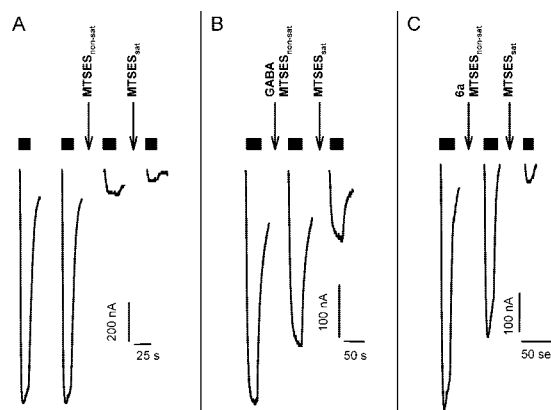
Figure 7. Protection assay shows that GABA and **6a** protect α_1F64Cβ_2 receptors from reaction with MTSES$^-$. (A) MTSES$^-$ modification of α_1F64Cβ_2 in the absence of agonist. Two GABA test pulses were applied to demonstrate the stability of the GABA current. At the downward arrow marked MTSES$_{nonsat}$, 10 μM MTSES$^-$ was applied for 12 s. Following washout, a GABA test pulse was recorded. The GABA test current (third trace) was reduced by 87%. At the downward arrow marked MTSES$_{sat}$, 20 μM MTSES$^-$ was applied for 50 s to bring the MTSES$^-$ reaction to completion. Following washout, a final GABA test pulse (fourth trace) was applied. Currents during MTSES$^-$ applications (↓) are not shown. (B) GABA protects α_1F64Cβ_2 from modification by MTSES$^-$. The same series of reagents are applied as in panel A, except that the MTSES$_{nonsat}$ was coapplied with 3.6 mM GABA. The GABA current elicited by the next GABA test pulse (middle trace) is significantly larger than the GABA current after the MTSES$_{nonsat}$ application in panel A, indicating that the presence of GABA significantly reduced the extent of reaction with the nonsaturating concentration of MTSES$^-$. (C) **6a** protects α_1F64Cβ_2 from modification by MTSES$^-$. The same series of reagents are applied as in panel A, except that the MTSES$_{nonsat}$ was coapplied with 10 mM **6a**. The GABA current elicited by the next GABA test pulse (middle trace) is significantly larger than the GABA current after the MTSES$_{nonsat}$ application in panel A, indicating that the presence of **6a** significantly reduced the extent of reaction with the nonsaturating concentration of MTSES$^-$. Currents during MTSES$^-$ application (↓) with or without agonist are not shown. Duration of application of GABA EC$_{50}$ test pulses are indicated by black horizontal bars above the current traces.

MTSEA-biotin resulted in 79 and 87% (n = 2) inhibition of the subsequent GABA test currents as compared to 87 and 100% (n = 2) inhibition in control experiments. For α_1R66C, the results of the protection experiments are complicated by the fact that **6a** reacts with α_1R66Cβ_2 as described below.

6a Reacts with the Engineered Cysteine in α_1R66Cβ_2 Receptors. To our surprise, while examining competition between GABA and **6a** on α_1R66Cβ_2 receptors, we noted that once the oocytes showed stable GABA test responses, coapplication of GABA and **6a** irreversibly reduced the subsequent GABA test currents (data not shown). Alternating between GABA and **6a** resulted in a progressive decline in the GABA test currents that finally led to a stable GABA current that was significantly lower, 68 ± 4% (n = 4), than the initial GABA test current (Figure 9A). At this stage, application of MTSES$^-$ caused no further effect. In contrast, application of MTSES$^-$ to α_1R66Cβ_2 expressing oocytes untreated with **6a** produced 62 ± 3% (n = 4) inhibition of GABA currents. Furthermore, the GABA currents after either **6a** or MTSES$^-$ application could be recovered by application of the reducing agent DTT (10 mM, 20 s) (Figure 9A). Theoretically, oxadiazole-2-thiones, such as **6a**, can exist in two tautomeric forms, the thio-amide (thione) form and the imino-thiol form. IR, UV, and NMR spectra indicate that they do exist predominantly in their thione form.[50] However, the ability to form the thiol-tautomer enables the
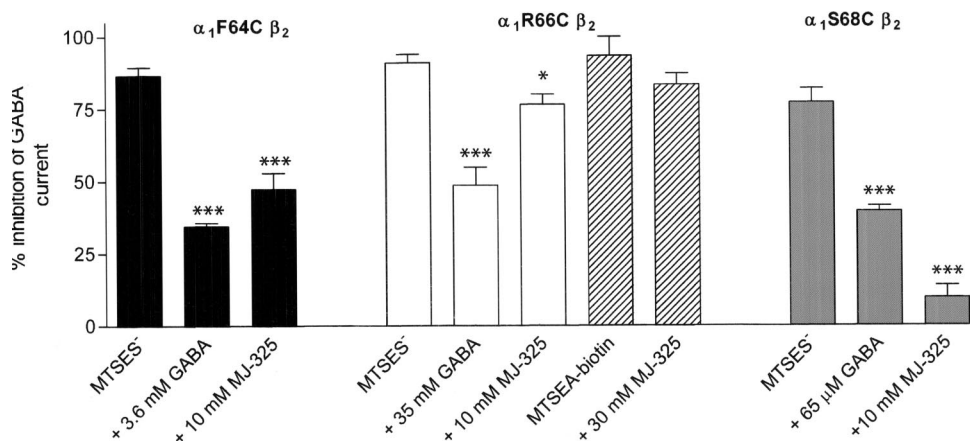
Figure 8. Summary of the protection assay with $\alpha_1F64C\beta_2$ (black bars), $\alpha_1R66C\beta_2$ (clear and striped bars), and $\alpha_1S68C\beta_2$ (gray bars). Bars indicate the average percent inhibition of GABA test currents following the application of a nonsaturating concentration of MTSES$^-$ either in the absence of agonist or in the presence of EC$_{90}$ GABA or **6a** (10 or 30 mM). We infer that a reagent, GABA or **6a**, protected a mutant from reaction with MTSES$^-$ if the extent of inhibition by MTSES$^-$ coapplied with either GABA or **6a** is significantly less than the extent of inhibition by MTSES$^-$ applied alone. Conditions where the coapplication of GABA or **6a** are significantly different than the effect of MTSES$^-$ application alone are indicated by * (* $P < 0.014$; *** $P < 0.0001$) by one way ANOVA and Fisher's PLSD. For $\alpha_1R66C\beta_2$, 30 μM MTSEA-biotin reduced the subsequent GABA test currents by 93%. Application of 30 μM MTSEA-biotin with 30 mM **6a** reduced the subsequent GABA test currents by 83%. The limited supply of **6a** precluded further experiments.
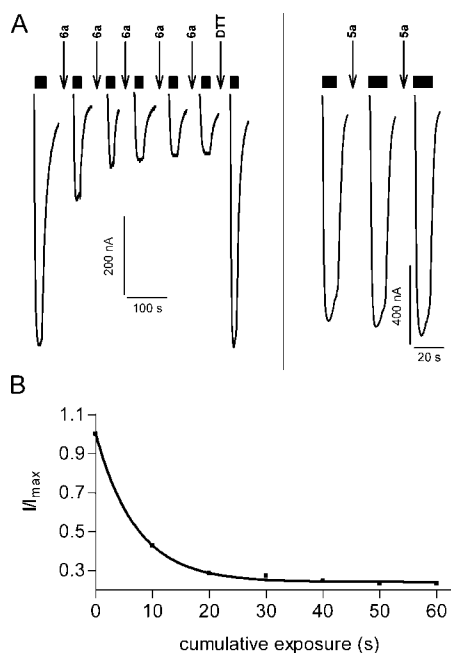

Figure 9. **6a** reacted with $\alpha_1R66C\beta_2$. (A) Currents recorded from an oocyte expressing $\alpha_1R66C\beta_2$. Alternating 10 s applications of 30 mM **6a** [indicated by (↓)] and 5.5 mM GABA test currents (bars above current traces) resulted in a progressive decrease in the GABA test currents. The decrease eventually plateaued, at which time a 12 s application of 10 mM MTSES$^-$ (↓) had no effect, indicating that all accessible cysteine had reacted with **6a**. Reduction by a 20 s application of 10 mM DTT (↓) led to complete recovery of the GABA test current magnitude. Currents during application of **6a**, MTSES$^-$, and DTT are not shown. (B) Application of the oxygen analogue **5a** (30 mM, 10 s) (↓) to an oocyte expressing $\alpha_1R66C\beta_2$ did not decrease the subsequent GABA test currents. Currents during **5a** application are not shown. (C) Reaction rate of **6a** with $\alpha_1R66C\beta_2$. GABA test currents were normalized to the initial GABA test current, plotted as a function of cumulative duration of **6a** application and fitted to a monoexponential decay function.

oxadiazole-2-thione to form a disulfide bond. Consistent with the idea of the formation of a stable disulfide bond, repeated 10 s applications of 30 mM **5a**, a **6a** analogue with an oxygen in place of the potentially sulfhydryl reactive oxadiazolethione

sulfur moiety, did not irreversible alter the subsequent GABA currents in $\alpha_1R66C\beta_2$ expressing oocytes (Figure 9B).

To measure the reaction rate of **6a** with α_1R66C, we alternately applied 5.5 mM GABA and **6a** to oocytes until the GABA currents no longer declined (Figure 9A). The decline in the $\alpha_1R66C\beta_2$ GABA currents as a function of the cumulative **6a** exposure time could be fit with a single exponential decay function. **6a** second-order reaction rate with the engineered cysteine in α_1R66C was 5 ± 1 M^{-1}/s ($n = 3$) (Figure 9A,C). The second-order reaction rate constant was independent of the **6a** concentration used (either 10 or 30 mM).

In our homology model based on the AChBP structure, the α_1 subunit residues R66 and T129 are in close proximity but on adjacent β-strands. On the basis of protection with agonist and antagonist SCAM analysis predicts that α_1T129 lines the binding pocket.[48] A 2 min application of 5 mM MTSES$^-$ reduced the subsequent currents elicited by GABA EC$_{50}$ test pulses in α_1T129Cβ_2 by $63 \pm 5\%$ ($n = 3$). We tested whether **6a** would react with α_1T129C. Alternate application of EC$_{50}$ GABA and 30 mM **6a** did not lead to a change in GABA EC$_{50}$ peak currents in α_1T129Cβ_2, α_1F64Cβ_2, or α_1S68Cβ_2 containing receptors, suggesting that the reaction of **6a** with α_1R66C is highly specific. It should be noted that the MTSES$^-$ reaction rate with α_1R66C was at least 5-fold slower than with any of the other cysteine mutants used in this study (Table 6). It was orders of magnitude slower than the reaction rate with α_1T129C. Thus, the lack of **6a** reaction with the other cysteine mutants is not due to lower intrinsic reactivity of those positions.

Discussion

Structure–Activity Relationships of 1,3,4-Oxadiazol-2-ones. The 1,3,4-oxadiazol-2-one compound with the highest affinity as measured by inhibiting muscimol binding is the aminomethyl-derivative **5d**, with IC$_{50}$ values of 1.4 μM and 1.1 μM against rat cortex and cerebellum, respectively. The homoderivative **5g** with its 2-aminoethyl side chain displayed seven times higher IC$_{50}$ values. The conversion of the primary amine function of **5d** to a secondary methylaminomethyl group in **5e** caused a significant decrease in affinity, and the tertiary dimethylami-nomethyl compound **9c** showed negligible capacity to displace [^{3}H]muscimol. Thus, the affinity among the 5-aminomethyl-

3H-[1,3,4]oxadiazol-2-ones decreases from the primary aminomethyl **5d** over the secondary methylaminomethyl **5g** to the tertiary dimethylaminomethyl **9c**. We infer that the amino group is involved in interactions with the binding site because the cyclohexyl-**9d** and methyl-**9e** substituted oxadiazol-2-ones that lack an amino group do not show significant inhibition of muscimol binding.

An additional steric demand at the methylene group of the aminomethyl compound **5d** that led to the 1-aminoethyl derivative **5f** was not well tolerated, i.e., the methyl group in **5f** led to a significant decrease in the ability to displace [³H]muscimol. The 2-pyrrolidine compound **5c**, which can be considered as a bridged aminomethyl derivative of **5d**, showed an almost complete loss of affinity. In **5c**, the inhibition reducing effects of a secondary amine function and a steric strain added to the methylene group are combined. Similarly, when the 2-aminoethyl side chain was incorporated into a 3-piperidyl ring as in **5b**, the compound was inactive. However, the 4-piperidyl compound **5a** was active although the IC_{50} was increased by a factor of 4 when compared to the 2-aminoethyl compound **5g**. Thus, the affinity appears to be sensitive to the position of the amino group because when it is at the 4 position in the piperidyl ring as in **5a**, the IC_{50} was 183 μM, but when located at the 3 position in **5b**, the affinity was negligible. Furthermore, derivatives of the 4-piperidyl amino group leading to tertiary amines in the form of the *N*-benzyl-piperidine **9b** or the *N*-methyl-piperidine **9a** showed weak activity in this assay. This is consistent with the loss of activity as the amino group transits from a primary to secondary to tertiary amino group.

Structure−Activity Relationships of 1,3,4-Oxadiazol-2-thiones. The 4-piperidyl derivative **6a** showed an IC_{50} comparable to the aminomethyl derivative **6d**. This is in contrast to the oxadiazolones, where the aminomethyl derivative showed a 40 times lower IC_{50} than the 4-piperidyl derivative. The aminoethyl derivative **6g** showed the third highest degree of inhibition in the thione series. However, when the aminomethyl or aminoethyl was bridged in the thione series to obtain a 2-pyrrolidinyl **6c** or 3-piperidinyl **6b** compound, a significant amount of affinity was still retained. This is also different from the oxadiazolones, where the corresponding modifications were not tolerated. Another difference was found when comparing the primary, secondary, and tertiary aminomethyl compounds. Here the primary aminomethyl **6d** had a higher affinity than the dimethylaminomethyl compound **10c**, which in turn had a higher affinity than the methylaminomethyl compound **6e**. This decline in affinity seems to be correlated to the basicity. We infer that the amine-N interacts with the protein. Other side chains that resulted in a weak affinity are the compounds with the 4-(*N*-methyl-piperidinyl) **10a** and the 4-(*N*-benzyl-piperidinyl) **10b** moiety. Again, the cyclohexyl- and methyl substituted oxadiazol-2-thiones **10d** and **10e** did not show a significant inhibition of muscimol binding.

Structure−Activity Relationships of Modifications to the 1,3,4-Oxadiazol-2-one Ring Itself. As mentioned above, substituting the 2-one oxygen with sulfur did not have a uniform effect. Depending on the amine-side chain in position 5 of the heterocycle, the sulfur bearing compound exhibited lower (4-piperidinyl, **6a** < **5a**; 3-piperidinyl, **6b** < **5b**; 2-pyrrolidinyl, **6c** < **5c**) or higher IC_{50} values (aminomethyl, **6d** > **5d**; 2-aminoethyl, **6g** > **5g**; methylaminomethyl, **6e** > **5e**) than their oxygen bearing counterparts. For other side chains, there was no difference in affinity detected between -thione and -one (*N*-methyl-piperidine, **9a** = **10a**; *N*-benzyl-piperidine, **9b** = **10b**). The 4-piperidinyl series **5a**, **6a**, **19** showed that the hydrogens

of the oxadiazol-2-one/oxadiazol-2-thione 3-nitrogen or of the tautomeric oxadiazol-2-ol/oxadiazol-2-thiol 2-alcohol/2 thioalcohol oxygen/sulfur are unlikely to be directly involved in hydrogen-bonding nor, in their deprotonated form, in ion−ion or ion−π interactions because the 2-methyl-1,3,4-oxadiazole showed intermediate affinity. Moreover, we infer that the heteroatoms in the 1,3,4-oxadiazol ring act as hydrogen-bond acceptors when interacting with amino acids in the binding site. However, the drop in affinity from **6a** over **19** to **5a** followed the decrease in volume of the 2-substituent of the 1,3,4-oxadiazol (sulfur > CH_3 > oxygen). The compound with the smallest substituent (hydrogen) at position 2 of the 1,3,4-oxadiazol **11** showed a complete loss of affinity opposite to the derivatives with an oxygen **9b** or sulfur **10b,** again indicating that some bulk at the 2-position is necessary.

The 1,2,4-triazoles explore the effect of substituting the oxygen at position 1 of the 1,3,4-oxadiazol-ones/thiones with a benzyl substituted nitrogen. This exchange was not tolerated at all in the aminomethyl compound: the triazole **16d** completely lost its affinity in contrast to the 1,3,4-oxadiazol-2-one, whereas the 4-piperidinyl triazole **16a** showed a reduced but still significant displacement of [³H]muscimol. The difference in tolerance of bulk at this position of the heterocyclic half of the compounds might indicate that the longer piperidine derivatives share the binding partners for the side chain amino-N with the shorter ligands but bridge to different amino acids of the binding site with the heterocyclic portion of the molecule. This difference in coordination might account for the difference in tolerance for bulky substituents.

Comparison with Previous 4-PIOL Derivatives. Frølund and colleagues have reported on the synthesis and evaluation of 4-PIOL derivatives as GABA partial agonists or antagonists. They mainly investigated the influence of substituents at position 4 of the 3-isoxazolol ring.[39,54] In these studies, small aliphatic and also bulky aromatic substituents were tolerated. 4-PIOL derivatives in these investigations had a K_i between 0.049 and 10 μM as compared to 4-PIOL with 9.1 μM and our best derivatives with an IC_{50} between 1 and 183 μM. Methyl or ethyl substitution of 4-PIOL lead to compounds that retained some agonistic activity with the binding affinity as determined by [³H]muscimol binding assays being retained as well, whereas the bulky substituents did not show agonistic activity, but their affinity was increased in the binding assays. In the context of the 1,3,4-oxadiazol-2-ol moiety used in the present study, substitution of the oxygen at position 1 with a benzyl substituted nitrogen did not improve affinity as **16a** had a somewhat lower affinity than **5a**. We infer that the large cavity that has been suggested to accommodate the aromatic residues of the 4-substituted 4-PIOL derivatives is not available for compounds of our series, possibly because the 1,3,4-triazol-2-ol derivatives are not arranged in a way that would align the aromatic moiety with the hydrophobic pocket. It is likely that the occupancy of this cavity by the aromatic substituted 4-PIOL derivatives prevents the binding site closure that has been proposed to be an early step in the conformational change linking ligand binding to channel gating.

It has been observed previously that the exchange of an oxygen in the small carboxyl group bioisosteric ring by a sulfur can have different effects: the sulfur analogue of 4-PIOL has a higher affinity than 4-PIOL, whereas the sulfur analogue of THIP has a lower affinity than the oxygen containing counterpart.[40,54,55] The conclusion was that the 3-isoxazolol heterocycles of 4-PIOL and THIP are not at identical positions in the binding sites. Further results demonstrated that the flexible

side chain of the arginine R66 in the α_1 subunit might enable the binding pocket to adapt to different bioactive conformations of ligands.[54]

α-Subunit Specificity. The electrophysiological characterization of the most active compounds was divided in investigating the agonistic potency of individual compounds and determining their modulating effect on GABA-induced currents. The agonistic profiling yielded **5d** as the most active compound. This compound had an EC_{50} comparable to the GABA EC_{50} at all $\alpha_{1-6}\beta_3\gamma_2$ subunit combinations, ranging from 30 μM for α_6 to 1 mM for α_3-containing receptors. In the GABA current modulating assay, **5d** showed potentiating effects at all subunit combinations reflecting its pure agonistic character. We assume that the small **5d** compound can be accommodated in all binding sites irrespective of the specific α subunit, where its orientation and size allow complete agonist-induced contraction of the binding site and subsequent gating in a manner comparable to the GABA induced effect. Increasing the spacer that bridges the basic amino function from the oxadiazolol moiety from a methylene group in **5d** to a piperidine ring in **5a** converts the compound from an unselective agonist into an antagonist at α_1, α_4, and α_6 containing receptors and a weak partial agonist at α_2, α_3 and α_5 containing receptors. The intrinsic activity is highest at α_5 containing receptors. The thio derivative of **5a**, **6a**, showed a comparable profile, with the exception that at α_2 containing receptors it is potentiating GABA currents at low concentrations while it is inhibitory at higher concentrations. The methyl derivative **19** was only agonistic at α_6 receptors, while it showed slight potentiating effects at high concentrations at α_2, α_4, α_5, and α_6 containing receptors.

6a Binds in the GABA Binding Site. Numerous drugs modulate and directly activate GABA$_A$ receptors often by binding to sites other than the GABA binding sites. On the basis of several lines of evidence, we conclude that **6a** binds within the GABA binding pocket. First, **6a** protected α_1F64C and α_1S68C from modification by MTSES$^-$ (Figures 7 and 8). These residues are located in the GABA binding site in a homology model based on the AChBP structure.[49,56–58] Czajkowski and co-workers previously showed that GABA protected the cysteine at α_1F64C from modification by MTSES$^-$ but pentobarbital did not. Pentobarbital activates the receptor by binding at a site in the transmembrane domain. Thus, the lack of protection by pentobarbital argues that the protection induced by GABA is due to local steric effects of GABA and not due to conformational changes associated with gating.[46,47] Thus, we conclude that **6a** protected α_1F64C by its presence in the GABA binding site and not by conformational changes induced by **6a** binding. Second, **6a** specifically and covalently modified the neighboring cysteine-substitution mutant, α_1R66C, inhibiting the subsequent GABA currents. This inhibition did not occur with **5a**, which has an oxygen in place of the thiol-reactive sulfur in **6a**. Furthermore, following inhibition of α_1R66C by reaction with **6a** subsequent application of MTSES$^-$ had no effect, whereas, without **6a** pretreatment, application of MTSES$^-$ would have inhibited the GABA-induced currents. Thus, MTSES$^-$ had no effect when it was applied after **6a** because MTSES$^-$ cannot react with disulfide linked sulfurs. In contrast, the inhibition induced by **6a** reaction was reversed by DTT application, indicating that **6a** formed a mixed disulfide bond with the cysteine thiol. Taken together, we infer that **6a** binds in the GABA binding site.

The ability of **6a** to protect α_1S68C from modification by MTSES$^-$ provides insight into the conformational changes induced by **6a** binding (Figure 8). Both GABA and pentobarbital

protected this cysteine mutant from MTSES$^-$ modification. Czajkowski and co-workers concluded that in the activated state conformation, access to this residue was reduced due to a conformational change of the binding site rather than by the presence of GABA in the binding site.[59] We infer that in the region of α_1S68, **6a** produces a similar conformational change to that induced by GABA and pentobarbital when it activates the receptor. This suggests that **6a** induces a conformational change in the receptor similar to that induced by GABA binding.

Further, the disulfide bond formation between **6a** and the introduced cysteine at the α_1R66 position provides insight into the orientation of **6a** in the GABA binding site. The reaction between **6a** and α_1R66C appears to be specific because **6a** did not react at a measurable rate with the cysteine substituted for the neighboring residues on the same β strand, α_1F64 or α_1S68, nor did it react with a cysteine at α_1T129, the residue predicted to lie in closest proximity on the adjacent β strand. If all other factors were similar, the ratio of the reaction rates of **6a** with the four cysteine mutants should be similar to the ratio of the reaction rates for the MTS reagents with these mutants. The MTS reagents reacted faster with α_1F64C and α_1S68C than with α_1R66C (Table 6). Thus, it is surprising that **6a** only reacted at a measurable rate with α_1R66C. Because **6a** is much less reactive than the MTS reagents, the reason why this compound only reacts at this position must be attributed to a highly selective interaction of the **6a** sulfur with the α_1R66C sulfur. Therefore, we infer that the favorable orientation of **6a** in the binding site brings the **6a** sulfur into close proximity with the α_1R66 position, leading to the highly specific reaction. This establishes one point of contact between **6a** and the complementary side of the binding site.

We assume that **6a** bridges the principle and complementary sides of the binding site in a manner similar to GABA. We generated a model of the GABA$_A$ receptor β_2–α_1 interface based on the AChBP crystal structure with nicotine bound (Figure 10). **6a** can fit into the binding site with its basic nitrogen superposed on the position of nicotine's basic pyridine nitrogen in the principle side of the binding site and with the **6a** sulfur in close proximity to the introduced $\alpha_1$66C sulfur on the complementary side of the binding site (Figure 10B). The close proximity of the sulfurs may explain the high collision probability and consequently the reactivity necessary to form the disulfide bond between **6a** and the engineered cysteine at position α_1R66. This orientation in the binding site may explain why it is a weak agonist. In the AChBP crystal structure on the complementary side of the binding site, nicotine forms hydrogen bonds with backbone carbonyls and amides on the β strand containing the residue that aligns with α_1T129 (Figure 10C). This β strand is adjacent to the α_1R66-containing β strand. **6a** is larger than GABA: the distance between the two potential H-bonding sites, i.e., the protonated positively charged nitrogen and the most distant high electron dense heteroatom O (GABA) and S (**6a**) (Figures 11 and 10) being 6.1 and 7.6 Å, respectively. Thus, GABA might only span the distance between the β-subunit principle site residues, where the positively charged N is coordinated and the α_1T129 β-strand of loop E (Figure 10A). In contrast, the larger **6a** extends to the more distant β strand containing residue α_1R66 (Figure 10B). Activation of the Cys-loop receptors may involve a contraction of the two halves of the binding site.[59] Because **6a** bridges to a different part of the complementary side of the binding site its ability to pull the two halves of the binding site together may be reduced compared to GABA, resulting in **6a** being a partial agonist. The idea that **6a** is a partial agonist because it is less effective at
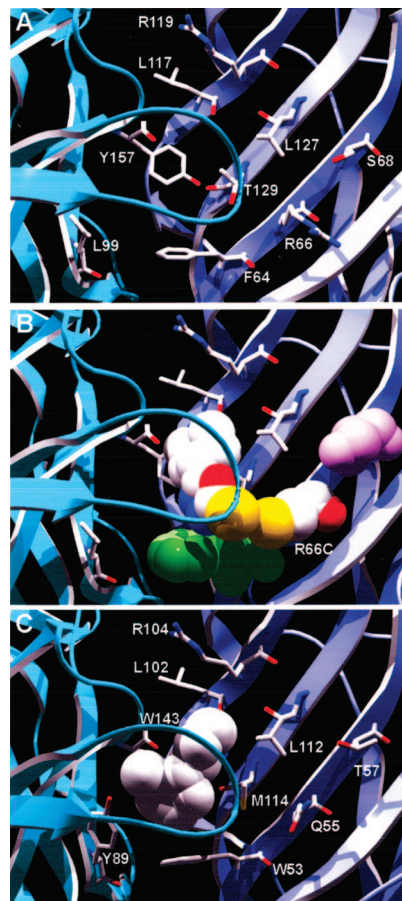
Figure 10. Homology model of the GABA_A receptor agonist binding site based on the AChBP structure (PDB 1UW6). (A) View of the principle side of the β_2 subunit GABA binding site (light blue) and of the complementary side of the α_1 subunit GABA binding site (dark blue), showing backbone in ribbon form. Side chains of residues mentioned in the text are shown in wire-frame format. (B) GABA binding site showing backbone in ribbon form with **6a** and α_1R66C shown in space-filling format with CPK colors. The close proximity of the sulfurs (yellow) in **6a** and α_1Cys66 is consistent with the observed reaction between **6a** and α_1Cys66. α_1F64 is shown in green space-filling format. The close proximity between α_1F64 and **6a** is consistent with the steric protection of the cysteine substituted at this position. In contrast, α_1S68 (pink-colored space-filling format) is not in close proximity to **6a**. (C) View of nicotine bound in the AChBP binding site (PDB 1UW6) from the same perspective as in panel B. Backbone is shown in ribbon form and nicotine in white-colored space-filling format. Side chains of AChBP residues aligned with the GABA_A cysteine mutants discussed in the text and shown in panel C are in wire-frame format. Nicotine interacts with the homologous β strand adjacent to the β strand containing the residue in this model aligned with GABA_A α_1R66.

closing the binding site is consistent with the conceptual model of partial agonism derived from structural studies of the ionotropic glutamate receptors.[60]

6a should not cover the α_1 loop connecting L117 and L127 that harbors the four amino acids (ITED in α_1) recently identified as α variant specific transducing elements rather than binding site elements.[4] A trap-like motion of this loop, to an extent specified by these four amino acids in a given α isoform, could further explain the differences in GABA sensitivities between the GABA_A receptor subtypes.

Conclusions

We synthesized a series of derivatives of 4-PIOL, a compound previously shown to be a weak GABA_A partial agonist. We
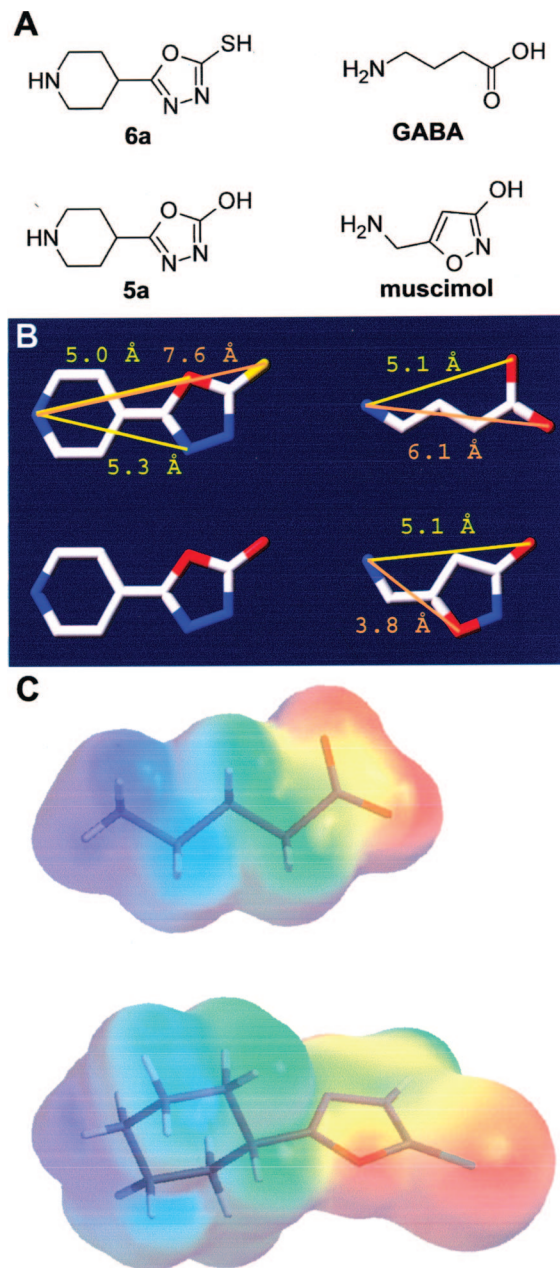

Figure 11. (A) Structures of **6a** and **5a** (left column) and of GABA and muscimol (right column). (B) Structures of the compounds in panel A with atomic distances between the basic nitrogen atom and other polar atoms in the respective molecules. Distances were measured after energy minimization (Chemsketch 5.12, ACD Inc., Toronto, Ontario, Canada). CPK color scheme used: carbon, white; nitrogen, blue; oxygen, red; sulfur, yellow. (C) Electrostatic potential mapped onto the van der Waals surface of GABA (top) and **6a** (bottom) with stick representation of molecules. Red indicates negative electrostatic potential and blue is positive potential. Image generated using Spartan. Note the similarity of the overall electrostatic potential, especially the distance between the positively charged nitrogen in GABA or **6a** to the negative carboxylate (GABA) or the oxadiazolthione moiety (**6a**).

started by replacing the 3-isoxazolol moiety in 4-PIOL with a 1,3,5-oxadiazol-2-ol moiety to yield **5a**. For the first time, we describe GABA_A receptor ligands with a 1,3,5-oxadiazol-2-ol as a carboxylic acid bioisosteric group. Compound **5a** was modified at different positions to investigate structure−activity relationships: the piperidine moiety was exchanged and modified, the substituent at the 2 position of the 1,3,5-oxadiazol-2-ol was varied, and the 1,3,5-oxadiazol-2-ol was exchanged by 1,2,4-triazol-5-ol.

The most active piperidine derivatives **5a** and **6a** were weak partial agonists that differentiated weakly between different α subunit containing receptors, whereas the small aminomethyl **5d** showed a profile of a pure agonist that is very similar to GABA.

The described structure−activity relationships extend the currently available information for ligands of the agonist binding site of the GABA$_A$ receptor. Frølund et al. have shown previously how to convert 4-PIOL into pure antagonistic compounds, while we now show how 4-PIOL can be modified to either obtain a pure or partial agonists with weak α subtype preferring profiles.

In addition, this study demonstrates that **6a** binds in the GABA binding site and that **6a** is oriented in the binding site such that its interaction with the complementary portion of the binding site is displaced from the interaction site of nicotine and carbamylcholine in the AChBP structure. The later finding may explain why **6a** is a partial agonist. Further investigations are necessary to determine if the two GABA binding sites are the only sites involved in the activity of this compound. These results coupled with GABA binding site homology models based on the AChBP structure may provide a foundation for rational design of GABA$_A$ receptor subtype-specific agonists with higher efficacy and specificity.

Experimental Section

Chemistry. Procedures and spectroscopic data for nontarget compounds can be found in the Supporting Information.

General Procedures for the Removal of the Boc-group: Procedure F (Compounds 5a,c,e,f,g, 6c,d,e,f,g, 16a,d, 17a, 19). The Boc-protected amine (1 equiv) was dissolved in a minimum amount of methanol and cooled in an ice-bath in a nitrogen atmosphere. After adding ethanolic HCl 2.3 N (4.5 equiv), the mixture was allowed to reach room temperature and stirred overnight. Products were isolated by filtration in a nitrogen atmosphere; in some cases, a precipitate was only formed after adding ethyl acetate (50−98%).

Procedure G (Compounds 5b,d, 6a,b, 19). The Boc-protected amine was dissolved in ethyl acetate and cooled to −20 °C in a nitrogen atmosphere. Gaseous HCl was bubbled through the mixture for 5 min. The reaction was allowed to come to room temperature and stirred until a precipitate was formed. Products were isolated by filtration in a nitrogen atmosphere or after removing the solvent and recrystallization in ethanol (56−88%).

5-Piperidin-4-yl-3*H*-[1,3,4]oxadiazol-2-one Hydrochloride (5a). Starting from **3a**, the compound was synthesized as described in procedure F: white crystals (98%); mp = 314 °C. ^{1}H NMR (DMSO-d_6) δ 1.74−1.88 (m, 2H, 2CH), 2.00−2.05 (m, 2H, 2CH), 2.89−3.03 (m, 3H, 3CH), 3.21−3.25 (m, 2H, 2CH), 8.98−9.28 (m, 2H, NH$_2$), 12.26 (s, 1H, NH). ^{13}C NMR (DMSO-d_6) δ 24.75 (CH$_2$), 30.94 (CH), 42.07 (CH$_2$), 155.11 (Cq), 158.08 (Cq). EI-MS *m/z* 169 (M$^+$). Anal. (C$_7$H$_{11}$N$_3$O$_2$·HCl) C, H, N.

5-Piperidin-3-yl-3*H*-[1,3,4]oxadiazol-2-one Hydrochloride (5b). Starting from **3b**, the compound was synthesized as described in procedure G. The solvent was removed under reduced pressure and the residue recrystallized from ethanol: white crystals (66%); mp = 207 °C. ^{1}H NMR (DMSO-d_6) δ 1.60−1.85 (m, 3H, 3CH), 1.97−2.01 (m, 1H, 1CH), 2.82−2.91 (m, 1H, 1CH), 2.96−3.04 (m, 1H, 1CH), 3.13−3.19 (m, 2H, 2CH), 9.26 (m, 2H, NH$_2$), 12.32 (s, 1H, NH). ^{13}C NMR (DMSO-d_6) δ 24.75 (CH$_2$), 30.94 (CH), 42.07 (CH$_2$), 155.11 (Cq), 158.08 (Cq). MS *m/z* 167 (M$^+$-2 free base). Anal. (C$_7$H$_{11}$N$_3$O$_2$·HCl) C, H, N.

L-5-Pyrrolidin-2-yl-3*H*-[1,3,4]oxadiazol-2-one Hydrochloride (5c). Starting from **3c**, the compound was synthesized as described in procedure F: white crystals (84%); mp = 199 °C. ^{1}H NMR (DMSO-d_6) δ 1.88−2.05 (m, 2H, 2CH), 2.12−2.30 (m, 2H, 2CH), 3.20−2.25 (m, 2H, 2CH), 4.63 (t, 7.75 Hz, 1H, CH), 10.13 (s, 2H, NH$_2$), 12.72 (s, 1H, NH). ^{13}C NMR (DMSO-d_6) δ 23.77 (CH$_2$),

27.18 (CH$_2$), 45.56 (CH$_2$), 52.88 (CH), 152.34 (Cq), 154.72 (Cq). EI-MS *m/z* 155 (M$^+$ free base); [α]^D = −3.9 ° (RT, *c* = 0.71, H$_2$O). Anal. (C$_6$H$_9$N$_3$O$_2$·HCl) C, H, N.

5-Aminomethyl-3*H*-[1,3,4]oxadiazol-2-one Hydrochloride (5d). Starting from **3d**, the compound was synthesized as described in procedure G. The product was separated by filtration after stirring a few minutes at room temperature: white crystals (88%); mp = 235 °C. ^{1}H NMR (DMSO-d_6) δ 4.03 (s, 2H, CH$_2$), 8.82 (s, 3H, CH$_2$NH$_3$), 12.71 (s, 1H, NH). EI-MS *m/z* 115 (M$^+$ free base). Anal. (C$_3$H$_5$N$_3$O$_2$·HCl) C, H, N.

5-Methylaminomethyl-3*H*-[1,3,4]oxadiazol-2-one Hydrochloride (5e). Starting from **3e**, the compound was synthesized as described in procedure F: white crystals (79%); mp = 176 °C. ^{1}H NMR (DMSO-d_6) δ 2.58 (s, 3H, CH$_3$), 4.15 (s, 2H, CH$_2$), 9.88 (s, 2H, NH$_2$), 12.81 (s, 1H, NH). ^{13}C NMR (DMSO-d_6) δ 32.75 (CH$_2$), 42.22 (CH$_3$), 150.10 (Cq), 154.65 (Cq). EI-MS *m/z* 129 (M$^+$ free base). Anal. (C$_4$H$_7$N$_3$O$_2$·HCl) C, H, N.

D-5-(1-Amino-ethyl)-3*H*-[1,3,4]oxadiazol-2-one Hydrochloride (5f). Starting from **3f**, the compound was synthesized as described in procedure F: white crystals (90%); mp = 194 °C. ^{1}H NMR (DMSO-d_6) δ 1.47 (d, 6.86 Hz, 3H, CH$_3$), 4.44 (q, 6.86 Hz, 1H, CH), 8.93 (2, 3H, NH$_3$), 12.75 (s, 1H, NH). ^{13}C NMR (DMSO-d_6) δ 15.77 (CH$_3$), 42.62 (CH$_2$), 154.16 (Cq), 154.67 (Cq). EI-MS *m/z* 129 (M$^+$ free base); [α]^D = +7.0 ° (RT, *c* = 0.63, H$_2$O). Anal. (C$_4$H$_7$N$_3$O$_2$·HCl) C, H, N.

[5-(2-Amino-ethyl-3*H*-[1,3,4]oxadiazol-2-one Hydrochloride (5g). Starting from **3g**, the compound was synthesized as described in procedure F: white crystals (77%); mp = 206 °C. ^{1}H NMR (DMSO-d_6) δ 2.89 (t, 6.60 Hz, 2H, *CH$_2$*CH$_2$NH$_3$), 3.06 (t, 6.74 Hz, 1H, CH$_2$*CH$_2$*NH$_3$), 8.23 (s, 3H, NH$_3$), 12.25 (s, 1H, NH). ^{13}C NMR (DMSO-d_6) δ 24.49 (CH$_2$), 35.37 (CH$_2$), 153.97 (Cq), 155.27 (Cq). EI-MS *m/z* 129 (M$^+$ free base). Anal. (C$_4$H$_7$N$_3$O$_2$·HCl) C, H, N.

5-Piperidin-4-yl-3*H*-[1,3,4]oxadiazol-2-thione Hydrochloride (6a). Starting from **4a**, the compound was synthesized as described in procedure G (74%). The compound was also synthesized following procedure F. In this case, $^1/_3$ of methanol cocrystallized with **6a**, which could be removed by solving the crystals in water, removing some of the solvent under vacuum at 20 °C and freeze-drying the resulting solution (91%): white crystals; mp = 232 °C. ^{1}H NMR (DMSO-d_6) δ 1.79−1.92 (m, 2H, 2CH), 2.06−2.12 (m, 2H, 2CH), 2.90−3.07 (m, 2H, 2CH), 3.15−3.28 (m, 3H, 3CH), 8.89−9.19 (m, 2H, NH$_2$), 14.49 (s, 1H, NH). ^{13}C NMR (DMSO-d_6) δ 24.96 (CH$_2$), 30.50 (CH), 42.01 (CH$_2$), 165.04 (Cq), 177.93 (Cq). EI-MS *m/z* 185 (M$^+$ free base). Anal. (C$_7$H$_{11}$N$_3$OS·HCl) C, H, N, S.

5-Piperidin-3-yl-3*H*-[1,3,4]oxadiazol-2-thione Hydrochloride (6b). Starting from **4b**, the compound was synthesized as described in procedure G, with the exception that 10% of the solvent were ethanol. The solvent was removed under reduced pressure and the residue recrystallized in ethanol: slightly green crystals (58%); mp = 219 °C. ^{1}H NMR (DMSO-d_6) δ 1.70−1.85 (m, 3H, 3CH), 2.00−2.10 (m, 1H, CH), 2.80−2.92 (m, 1H, CH), 3.04−3.19 (m, 2H, 2CH), 3.34−3.43 (m, 2H, 2CH), 9.20−9.60 (m, 2H, NH$_2$), 14.55 (s, 1H, NH). ^{13}C NMR (DMSO-d_6) δ 20.75 (CH$_2$), 24.88 (CH$_2$), 30.82 (CH), 43.02 (CH$_2$), 44.01 (CH$_2$), 163.08 (Cq), 177.94 (Cq). EI-MS *m/z* 185 (M$^+$ free base). Anal. (C$_7$H$_{11}$N$_3$OS·HCl·$^1/_3$H$_2$O) C, H, N, S.

L-5-Pyrrolidin-2-yl-3*H*-[1,3,4]oxadiazol-2-thione Hydrochloride (6c). Starting from **4c**, the compound was synthesized as described in procedure F: white crystals (50%); mp = 167 °C. ^{1}H NMR (DMSO-d_6) δ 1.91−2.08 (m, 2H, 2CH), 2.15−2.36 (m, 2H, 2CH), 3.26 (app t, 6.44 Hz, 2H, 2CH), 4.80 (app t, 7.23 Hz, 2H, 2CH), 10.15 (s, 1H, NH). ^{13}C NMR (DMSO-d_6) δ 23.79 (CH$_2$), 27.73 (CH$_2$), 45.71 (CH$_2$), 52.13 (CH), 159.25 (Cq), 178.38 (Cq). EI-MS *m/z* 171 (M$^+$ free base); [α]^D = −0.14 ° (RT, *c* = 0.58, H$_2$O). Anal. (C$_6$H$_9$N$_3$OS·HCl·$^1/_3$H$_2$O) C, H, N, S.

5-Aminomethyl-3*H*-[1,3,4]oxadiazol-2-thione Hydrochloride (6d). Starting from **4d**, the compound was synthesized as described in procedure F: beige crystals (71%); mp = 184 °C. ^{1}H NMR (DMSO-d_6) δ 4.21 (s, 2H, CH$_2$), 8.93 (s, 3H, NH$_3$), 14.83 (s, 1H, NH). ^{13}C NMR (DMSO-d_6) δ 33.56 (CH$_2$), 158.27 (Cq), 178.21 (Cq). EI-MS *m/z* 131. Anal. (C$_3$H$_5$N$_3$OS·HCl) C, H, N, S.

5-Methylaminomethyl-3*H*-[1,3,4]oxadiazol-2-thione Hydrochloride (6e). Starting from **4e**, the compound was synthesized as described in procedure F: white crystals (81%); mp = 158 °C. ^{1}H NMR (DMSO-d_6) δ 2.61 (s, 3H, CH$_3$), 4.35 (s, 2H, CH$_2$), 9.99 (s, 1H, NH). ^{13}C NMR (DMSO-d_6) δ 32.96 (CH$_3$), 41.51 (CH$_2$), 156.95 (Cq), 178.22 (Cq). EI-MS *m/z* 145 (M$^+$). Anal. (C$_4$H$_7$N$_3$OS·HCl) C, H, N, S.

[5-(2-Amino-ethyl)-3*H*-[1,3,4]oxadiazol-2-thione Hydrochloride (6g). Starting from **4g**, the compound was synthesized as described in procedure F: white crystals (94%); mp = 222 °C. ^{1}H NMR (DMSO-d_6) δ 3.06−3.14 (m, 4H, CH$_2$CH$_2$), 8.26 (s, 3H, NH$_3$), 14.48 (s, 1H, NH). ^{13}C NMR (DMSO-d_6) δ 23.85 (CH$_2$), 35.49 (CH$_2$), 161.02 (Cq), 178.14 (Cq). EI-MS *m/z* 145 (M$^+$ free base). Anal. (C$_4$H$_7$N$_3$OS·HCl) C, H, N.

General Procedures for the Synthesis of Oxadiazol-2-ones: Procedure H (Compounds 9a−c). The tertiary amine (2 equiv) was dissolved in CH$_2$Cl$_2$ and cooled to 0 °C under a nitrogen atmosphere. After adding a solution of carbonic acid bis(trichloromethyl) carbonate (1 equiv) in CH$_2$Cl$_2$ dropwise, the mixture was refluxed. The reaction mixture was evaporated to dryness and the residue recrystallized or chromatographed (20−55%).

5-(1-Methyl-piperidin-4-yl)-3*H*-[1,3,4]oxadiazol-2-one (9a). Starting from **8a**, the compound was synthesized as described in procedure H and recrystallized from methanol: white crystals (55%); mp = 281 °C. ^{1}H NMR (DMSO-d_6) δ 1.84−1.98 (m, 2H, 2CH), 2.05−2.15 (m, 2H, 2CH), 2.69 (s, 3H, CH$_3$), 2.84−3.03 (m, 3H, 2CH), 3.14−3.44 (m, 2H, 2CH), 10.76 (s, 1H, NH), 12.25 (s, 1H, NH). EI-MS *m/z* 183 (M$^+$ free base). Anal. (C$_8$H$_{13}$N$_3$O$_2$·HCl·1/2H$_2$O) C, H, N.

5-(1-Benzyl-piperidin-4-yl)-3*H*-[1,3,4]oxadiazol-2-one Hydrochloride (9b). Starting from **8b**, the compound was synthesized as described in procedure H and recrystallized from methanol: white crystals (55%); mp = 253 °C. The NMR- and MS-data agreed with literature.[61] Anal. (C$_{14}$H$_{17}$N$_3$O$_2$·HCl) C, H, N.

5-Dimethylaminomethyl-3*H*-[1,3,4]oxadiazol-2-one (9c). Starting from **8c**, the compound was synthesized as described in procedure H. The mixture was poured onto water and extracted with ethyl acetate at pH 7. The combined organic extracts were dried (Na$_2$SO$_4$), the solvent was removed under vacuo, and the residue chromatographed with ethyl acetate: white crystals (20%); mp = 103 °C; R_f (ethyl acetate): 0.09. ^{1}H NMR (DMSO-d_6) δ 2.18 (s, 6H, N(CH$_3$)$_2$), 3.36 (s, 2H, CH$_2$), 12.22 (s, 1H, NH). ^{13}C NMR (DMSO-d_6) δ 44.72 (2CH$_3$), 53.52 (CH$_2$), 154.76 (Cq), 155.27 (Cq). EI-MS *m/z* 143 (M$^+$). Anal. (C$_5$H$_9$N$_3$O$_2$) C, H, N.

5-Cyclohexyl-3*H*-[1,3,4]oxadiazole-2-one (9d). Starting from **8d**, compound **9d** was prepared according to procedure H and chromatographed: colorless oil which crystallizes on standing (85%); mp = 29 °C. IR data agreed with literature.[62] R_f (petroleum ether/ethyl acetate = 2/1): 0.5. ^{1}H NMR (DMSO-d_6) δ 1.13−1.43 (m, 5H, 5CH), 1.58−1.70 (m, 3H, 3CH), 1.85−1.88 (m, 2H, 2CH), 2.53−2.62 (m, 1H, CH), 12.03 (s, 1H, NH). ^{13}C NMR (DMSO-d_6) δ 24.45 (2CH$_2$), 25.07 (CH$_2$), 28.45 (2CH$_2$), 34.63 (CH), 154.89 (Cq), 159.71 (Cq). EI-MS *m/z* 168 (M$^+$). Anal. (C$_8$H$_{12}$N$_2$O$_2$·^{1}/$_5$H$_2$O) C, H, N.

5-Methyl-3*H*-[1,3,4]oxadiazole-2-one (9e). Starting from **8e**, compound **9e** was prepared according to procedure H and recrystallized from CH$_2$Cl$_2$ and *n*-hexane: white crystals (67%); mp = 112 °C.[63] ^{13}C NMR-data agreed with literature.[50] ^{1}H NMR (DMSO-d_6) δ 2.18 (s, 3H, CH$_3$), 11.99 (s, 1H, NH). EI-MS *m/z* 101 (M$^+$ + 1). Anal. (C$_3$H$_4$N$_2$O$_2$) C, H, N.

5-(1-Methyl-piperidin-4-yl)-3*H*-[1,3,4]oxadiazole-2-thione (10a). A mixture of **8a** (1 equiv), pyridine (1.6 mL/equiv), and CS$_2$ (0.2 mL/equiv) was treated at 80−90 °C until the evolution of H$_2$S had stopped. After removing the solvent under reduced pressure, the residue was recrystallized in ethanol and subsequently in methanol. The compound was chromatographed and again recrystallized from methanol: beige crystals (17%); mp = 248 °C; R_f (methanol): 0.5. ^{1}H NMR (DMSO-d_6) δ 1.71−1.84 (m, 2H, 2CH), 2.00−2.10 (m, 2H, 2CH), 2.61 (s, 3H, CH$_3$), 2.75−2.95 (m, 3H, 3CH), 3.18−3.27 (m, 2H, 2CH). ^{13}C NMR (DMSO-d_6) δ 26.99 (2CH$_2$), 30.54 (CH),

43.72 (CH$_3$), 53.02 (2CH$_2$), 164.41 (Cq), 178.93 (Cq). EI-MS *m/z* 199 (M$^+$). Anal. (C$_8$H$_{13}$N$_3$OS) C, H, N, S.

5-(1-Benzyl-piperidin-4-yl)-3*H*-[1,3,4]oxadiazole-2-thione (10b). Compound was synthesized according to the synthesis described for compound **10a** starting from **8b**: slightly beige crystals (34%); mp = 220 °C; R_f (chloroform/methanol = 4/1): 0.4. The NMR- and MS-data agreed with literature.[61] Anal. (C$_{14}$H$_{17}$N$_3$OS) C, H, N, S.

5-Dimethylaminomethyl-3*H*-[1,3,4]oxadiazole-2-thione (10c). Starting from **8c**, the compound was synthesized as described in procedure E. The mixture was poured onto water and extracted with ethyl acetate at pH 7. The combined organic extracts were dried (Na$_2$SO$_4$), the solvent was removed under vacuo, and the residue chromatographed: beige crystals (5%); mp = 119 °C; R_f (ethyl acetate): 0.08. ^{1}H NMR (DMSO-d_6) δ 7.45 (d, 1H, IndH), 2.31 (s, 6H, N(CH$_3$)$_2$), 3.71 (s, 2H, CH$_2$). ^{13}C NMR (DMSO-d_6) δ 44.38 (CH$_3$), 52.11 (CH$_2$), 53.02 (2CH$_2$), 160.35 (Cq), 178.80 (Cq). EI-MS *m/z* 159 (M$^+$). Anal. (C$_5$H$_9$N$_3$OS) C, H, N.

5-Cyclohexyl-3*H*-[1,3,4]oxadiazole-2-thione (10d). Starting from **8d**, compound **10d** was prepared according to procedure E and chromatographed: slightly yellow crystals (46%); mp = 81 °C; R_f (petroleum ether/ethyl acetate = 5/1): 0.3. ^{1}H NMR (DMSO-d_6) δ 1.14−1.48 (m, 5H, 5CH), 1.57−1.71 (m, 3H, 3CH), 1.90−1.93 (m, 2H, 2CH), 2.74−2.84 (m, 1H, CH), 14.32 (s, 1H, NH). ^{13}C NMR (DMSO-d_6) δ 24.79 (2CH$_2$), 25.34 (CH$_2$), 29.05 (2CH$_2$), 34.44 (CH), 167.10 (Cq), 177.87 (Cq). EI-MS *m/z* 184 (M$^+$). Anal. (C$_8$H$_{12}$N$_2$OS) C, H, N.

5-Methyl-3*H*-[1,3,4]oxadiazole-2-thione (10e). Starting from **8e**, compound **10e** was prepared according to procedure E, and chromatographed: white crystals (17%); mp = 78 °C;[64] R_f (petroleum ether/ethyl acetate = 5/1): 0.1. NMR data agreed with literature.[65] EI-MS *m/z* 117 (M$^+$ + 1). Anal. (C$_3$H$_4$N$_2$OS) C, H, N.

General Procedures for the Synthesis of [1,3,4]Oxadiazols: Procedure I (Compounds 11, 18). The hydrazide was refluxed for two hours in excess triethoxyalkane. Afterward, alcohol, which is formed during the reaction, was removed by distillation. The residue was refluxed for 5 h. After cooling to RT, the mixture was treated with water, saturated with K$_2$CO$_3$, and extracted several times with ethyl acetate. The combined organic extracts were dried (Na$_2$SO$_4$), evaporated and chromatographed (62−66%).

1-Benzyl-4-[1,3,4]oxadiazol-2-yl-piperidine (11). Starting from **8b** and triethoxyethane, the compound was prepared according to procedure I and chromatographed starting with petroleum ether/ethyl acetate = 1/1 and switching to methanol/ethyl acetate = 1/1: white slightly beige crystals (62%); mp = 61 °C; R_f (ethyl acetate/petroleum ether = 1/1): 0.1; R_f (methanol/ethyl acetate = 1/1): 0.4. ^{1}H NMR (DMSO-d_6) δ 1.64−1.77 (m, 2H, 2CH), 1.90−2.00 (m, 2H, 2CH), 2.03−2.11 (m, 2H, 2CH), 2.74−2.84 (m, 2H, 2CH), 2.89−2.99 (m, 1H, CH), 3.45 (s, 2H, CH$_2$−Ph), 7.18−7.32 (m, 5H, CH$_{Ar}$), 9.13 (s, 1H, CH$_{Oxadiazole}$). ^{13}C NMR (DMSO-d_6) δ 29.32 (2CH$_2$), 32.55 (CH), 52.31 (2CH$_2$), 62.56 (CH$_2$), 127.17 (CH), 128.45 (2CH), 129.05 (2CH), 138.63 (Cq), 154.46 (CH), 168.67. EI-MS *m/z* 244 (M$^+$). Anal. (C$_{14}$H$_{17}$N$_3$O) C, H, N.

4-Benzyl-5-piperidin-4-yl-2,4-dihydro-[1,2,4]triazol-3-one Hydrochloride (16a). Starting from **14a**, compound **16a** was synthesized as described in procedure F: white crystals (66%); mp = 251 °C. ^{1}H NMR (DMSO-d_6) δ 1.65−1.80 (m, 4H, 4CH), 2.77−2.95 (m, 3H, 3CH), 3.15−3.25 (m, 2H, 2CH), 4.81 (s, 2H, CH$_2$−Ph), 7.21−7.37 (m, 5H, CH$_{Ar}$), 8.85−9.25 (m, 2H, NH$_2$), 11.70 (s, 1H, NH). ^{13}C NMR (DMSO-d_6) δ 26.29 (2CH$_2$), 30.21 (CH), 42.48 (2CH$_2$), 43.36 (CH$_2$), 78.44 (Cq), 127.19 (2CH), 127.89 (CH), 129.03 (2CH), 137.31 (Cq), 149.47 (Cq), 155.30 (Cq). EI-MS *m/z* 258 (M$^+$). Anal. (C$_{13}$H$_{19}$N$_4$O·HCl·^{5}/$_4$H$_2$O) C, H, N.

5-Aminomethyl-4-benzyl-2,4-dihydro-[1,2,4]triazol-3-one (16d). Starting from **12d**, compound **16a** was synthesized as described in procedure L; because no precipitate was formed, the mixture was extracted with several portions of ethyl acetate. The combined organic extracts were dried (Na$_2$SO$_4$) and the solvent evaporated under vacuo until the crystallization started: white crystals (44%); mp = 150 °C. ^{1}H NMR (DMSO-d_6) δ 1.78 (s, 2H, NH$_2$), 3.44 (s,

2H, CH$_2$N), 4.86 (s, 2H, CH$_2$–Ph), 7.22–7.37 (m, 5H, CH$_{Ar}$), 11.55 (s, 1H, NH). ^{13}C NMR (DMSO-d_6) δ 37.76 (CH$_2$), 43.30 (CH$_2$), 127.35 (2CH), 127.80 (CH), 128.96 (2CH), 137.38 (Cq), 148.79 (Cq), 155.73 (Cq). EI-MS *m/z* 204 (M$^+$). Anal. (C$_{10}$H$_{12}$N$_4$O) C, H, N.

4-Benzyl-5-piperidin-4-yl-2,4-dihydro-[1,2,4]triazol-3-thione Hydrochloride (17a). Starting from **15**, compound **17a** was synthesized as described in procedure F: white crystals (95%); mp = 285 °C. ^{1}H NMR (DMSO-d_6) δ 1.63–1.78 (m, 4H, 4CH), 2.79–2.91 (m, 2H, 2CH), 2.98–3.08 (m, 1H, CH), 3.14–3.22 (m, 2H, 2CH), 5.27 (s, 2H, CH$_2$-Ph), 7.26–7.37 (m, 5H, CH$_{Ar}$), 8.68–9.04 (m, 2H, NH$_2$), 13.83 (s, 1H, NH). ^{13}C NMR (DMSO-d_6) δ 26.64 (2CH$_2$), 30.31 (CH), 42.49 (2CH$_2$), 45.91 (CH$_2$), 127.36 (2CH), 128.12 (CH), 129.03 (2CH), 136.29 (Cq), 154.60 (Cq), 167.43 (Cq). EI-MS *m/z* 274 (M$^+$). Anal. (C$_{14}$H$_{18}$N$_4$S·HCl·$^5/_4$H$_2$O) C, H, N, S.

5-Aminomethyl-4-benzyl-2,4-dihydro-[1,2,4]triazol-3-thione (17d). Starting from **13d**, compound **17d** was synthesized as described in procedure L and chromatographed with petroleum ether/ethyl acetate = 1/3 to wash off most of the intermediate BOC-protected triazole-3-thione and then with ethyl acetate/methanol = 1/5 and subsequently with CHCl$_3$/methanol = 4/1: white crystals (11%); mp = 69 °C; R_f (CHCl$_3$/methanol = 4/1): 0.52; white crystals (11%); mp = 158 °C. ^{1}H NMR (DMSO-d_6) δ 2.07 (s, 2H, NH$_2$), 3.15 (s, 1H, NH), 3.55 (s, 2H, *CH$_2$*NH$_2$), 5.32 (s, 2H, CH$_2$–Ph), 7.26–7.39 (m, 5H, CH$_{Ar}$). ^{13}C NMR (DMSO-d_6) δ 37.23 (CH$_2$), 45.71 (CH$_2$), 127.39 (2CH), 128.02 (CH), 128.98 (2CH), 136.24 (Cq), 153.74 (Cq), 167.89 (Cq). EI-MS *m/z* 220 (M$^+$). Anal. (C$_{10}$H$_{12}$N$_4$S·$^9/_{10}$H$_2$O) C, H, N, S.

4-(5-Methyl-[1,3,4]oxadiazol-2-yl)-piperidine Hydrochloride (19). Starting from **18**, the compound was synthesized as described in general procedure G (56%); the corresponding hydrobromide was obtained by stirring 2.6 mmol of **18** in 1 mL of HBr in acetic acid (5.7 M) under a nitrogen atmosphere overnight (98%). Analytical data for the hydrochloride: mp = 193 °C. ^{1}H NMR (DMSO-d_6) δ 1.85–1.99 (m, 2H, 2CH), 2.09–2.14 (m, 2H, 2CH), 2.45 (s, 3H, CH$_3$), 2.94–3.05 (m, 2H, 2CH), 3.22–3.33 (m, 3H, 3CH), 9.11–9.35 (m, 2H, NH$_2$). ^{13}C NMR (DMSO-d_6) δ 10.80 (CH$_3$), 25.66 (2CH$_2$), 30.24 (CH), 42.13 (2CH$_2$), 163.98 (Cq), 167.68 (Cq). Anal. (C$_8$H$_{13}$N$_3$O·HCl·$^5/_3$H$_2$O) C, H, N.

[^{3}H]Muscimol Ligand Binding Assays. Adult male Sprague–Dawley rats (supplied by the Department of Laboratory Animals, University of Mainz) were decapitated, their brains removed, and cerebellum and cortex separated. The tissue was homogenized in 50 mM Tris/citrate, pH 7.3, in an Ultraturrax (IKA, Staufen, Germany) for 15 s. The membranes were centrifuged at 43000*g* for 20 min. The washing step was repeated four times before the membranes were frozen at −20 °C. After slow thawing, the washing steps were repeated another two times and frozen again until use. Before each experiment, the membranes were recentrifuged and diluted to the desired protein concentration. Resuspended cell membranes (50–200 µg protein per tube) were incubated in a final volume of 0.5 mL of 50 mM Tris/citrate buffer, pH 7.3, for [^{3}H]muscimol binding (6 nM) with and without the novel compounds in the concentration range given in the text. Nonspecific binding was determined in the presence of 100 µM GABA. After 60 min on ice, the assay mixtures were rapidly diluted to 5 mL with ice-cold 10 mM Tris/HCl, pH 7.4, filtered through glass fiber filters (no. 52, Schleicher & Schuell, Dassel, Germany) and washed once with 5 mL 10 mM Tris/HCl, pH 7.4. Filters were immersed in 4 mL of Zinsser AquaSolv (Munich, Germany) scintillation fluid, and the radioactivity determined in a Beckman liquid scintillation counter using external standardization. Statistical calculations were performed using the Graph Pad Prism program (GraphPad Software, San Diego, CA.) with and without the novel compounds.

Cell Culturing and Cell Transfection. For electrophysiological recording, HEK-293 cells were passaged and replated on 12-mm glass coverslips located in 9.6-cm plastic dishes filled with 10 mL of Minimum Essential Medium (MEM, Gibco) supplemented with 158 mg/L sodium bicarbonate, 2 mM glutamine (Gibco), 100 U/mL penicillin-streptomycin (Gibco), and 10% fetal calf serum (Gibco).

Cultures were maintained at 37 °C in a humidified 95% O$_2$/5% CO$_2$ atmosphere for 2–3 days.

Transfection with recombinant rat GABA$_A$ receptors were carried out as described in detail.[66,67] Briefly, HEK 293 cells were transfected using the calcium phosphate precipitation method with rat GABA$_A$ receptor cDNAs in eukaryotic expression vectors[68] for the α, β, and γ subunits. For optimal receptor expression, final concentrations (µg vector DNA per 9.6 cm tissue culture plate) were: α_1, 2; α_2 4.8; α_3, 1.2; α_4 10; α_5, 0.8; α_6, 2; β_3, 0.4; and γ_2S, 0.3. The γ_2S variant is abbreviated γ_2 in the remainder of the text. To identify transfected cells, all subunit combinations were cotransfected with 1 µg per plate of pNI-EGFP.

HEK293 Electrophysiology. Two days after transfection, single coverslips containing HEK 293 cells were placed in a recording chamber mounted on the movable stage of a fluorescence microscope (Olympus IX70) and perfused with a defined saline solution containing (in mM): 130 NaCl, 5.4 KCl, 2 CaCl$_2$, 2 MgSO$_4$, 10 glucose, 5 sucrose, and 10 HEPES (free acid), pH adjusted to 7.35 with NaOH. Transfected cells were identified by their green fluorescence due to the expression of the pNI-EGFP vector. Ligand-mediated membrane currents from these cells were studied using the whole-cell patch-clamp recording technique.[69] Patch pipettes were pulled from hard borosilicate capillary glass (0.5 mm i.d., 1.5 mm o.d., Vitrex, Science Products GmbH, Hofheim, Germany) using a horizontal puller (Sutter Instruments, CA, model P-97) in a multistage process. The pipettes had an initial resistance of 2−4 MΩ when filled with a solution containing (in mM): 90 KCl, 50 KOH, 2 CaCl$_2$, 2 MgCl$_2$, 10 EGTA, 3.1 ATP (dipotassium salt), 0.4 GTP (trisodium salt), and 10 HEPES (free acid), pH 7.35.

The junction potential between the pipet and the external solution was less than 2.3 mV and therefore was neglected. Seal resistances >1 GΩ were routinely obtained by applying gentle suction to the pipettes. Membrane rupture was monitored electrically as an increase in capacitance. Pipette capacitance, membrane capacitance, and series resistance were electronically compensated to minimize capacitive transients. A series resistance compensation of >60% was regularly used.

To analyze modulations of the GABA-induced currents, the approximate receptor subtype specific GABA EC$_{20}$ and increasing drug concentrations were applied to the cells using a fast perfusion stepper system (SF-77B, Perfusion Fast Step, Warner Instruments, Inc., Hamden, CT). In the case of **5a** and **6a**, the following concentrations were coapplied (in µM): 0.1, 1, 10, 100, 1000; for **19** and **5d**, the concentration range used was (in µM): 0.1, 0.3, 1, 3, 10, 30, 100, 300, 1000. Additionally, the intrinsic activity of all compounds was tested by applying them alone to the cells in concentrations of 1, 10, 100, and 1000 µM.

Responses of cells were recorded by patch-clamp amplifier (EPC-8, HEKA-Electronic, Lambrecht, Germany) in conjunction with a standard personal computer and the pClamp 8.1 software package (Axon Instruments, Foster City, CA). The standard holding-potential for the cells was −40 mV. Whole cell currents were low-pass filtered by a eight-pole Bessel filter at 5 or 3 kHz before being digitized by a Digidata 1322A interface (Axon Instruments, Foster City, CA) and recorded by the computer at a sampling rate of at least 5 kHz.

Mutagenesis and Oocyte Expression. The rat GABA$_A$ receptor α_1 and β_2 subunit DNA constructs in the pGH19 vector (α_1 wild-type (wt), α_1F64C, α_1R66C, α_1S68C, α_1T129C, β_2 wt) were obtained from Dr. Cynthia Czajkowski, University of Wisconsin−Madison. Their identity was verified by restriction digestion and DNA sequencing. Plasmids were linearized with NheI prior to in vitro mRNA transcription with T7 RNA polymerase (Amplicap T7 High Yield Message MakerTM, Epicenter Technologies, Madison, WI). mRNA was dissolved in diethylpyrocarbamate-treated water and stored at −80 °C. Female *Xenopus laevis* were purchased from Nasco Science (Fort Atkinson, WI). Stage V−VI oocytes were defolliculated with a 75 min treatment with 2 mg/mL type 1A collagenase (Sigma Chemical Co., St. Louis, MO) in OR2 (82.5 mM NaCl, 2 mM KCl, 1 mM MgCl$_2$, and 5 mM HEPES; pH adjusted to 7.5 with NaOH). Oocytes were washed thoroughly in

OR2 and kept in SOS medium (82.5 mM NaCl, 2.5 mM KCl, 1 mM MgCl$_2$, 5 mM HEPES, pH 7.5) supplemented with 1% antibiotic-antimycotic (100×) liquid (10000 IU/mL penicillin, 10000 μg/mL streptomycin, and 25 μg/mL of amphotericin B; Invitrogen, Carlsbad, CA) and 5% horse serum (Sigma). Oocytes were injected 24 h after isolation with 50 nL (10 ng) of a 1:1 mixture of rat α_1:β_2 subunit mRNA and were kept in horse serum medium for 2−10 days at 17 °C. Mutant subunit mRNA was substituted for wt α_1 subunit where necessary.[70]

Two-Electrode Voltage Clamp Recording. The electrophysiological recordings were conducted at room temperature in a ∼250 μL chamber continuously perfused at a rate of 5−6 mL/min with Ca^{2+}-free frog Ringer buffer (CFFR; 115 mM NaCl, 2.5 mM KCl, 1.8 mM MgCl$_2$, 10 mM HEPES pH 7.5 with NaOH) using equipment and procedures described previously.[52] Currents were recorded from individual oocytes using two-electrode voltage-clamp at a holding potential of −60 mV. The ground electrode was connected to the bath via a 3 M KCl/Agar bridge. Glass microelectrodes had a resistance of <2 MΩ when filled with 3 M KCl. Data were acquired and analyzed using a TEV-200 amplifier (Dagan Instruments, Minneapolis, MN), a Digidata 1200 or Digidata 1322A data interface (Axon Instruments, Union City, CA), and pClamp 7 or pClamp 8 software (Axon Instruments). Currents (I_{GABA}) were elicited by applications of GABA separated by at least 5 min of CFFR wash to allow complete recovery from desensitization. Currents were judged to be stable if the variation between consecutive GABA pulses was <10%.

Reagents. The sulfhydryl-reactive methanethiosulfonate (MTS) reagents used in these experiments were 2-sulfonatoethyl methanethiosulfonate (MTSES$^-$) and 2-((biotinoyl)amino)ethyl methanethiosulfonate (MTSEA-biotin) (Biotium, Inc., Hayward, CA). MTS-reagents react with cysteine (Cys) and covalently couple a 2-sulfonatoethylsulfide (MTSES$^-$) or a 2-((biotinoyl)amino)ethylsulfide moiety (MTSEA-biotin) onto protein sulfhydryls. A 100 mM stock solution of MTSES$^-$ in water or MTSEA-biotin in DMSO was prepared daily and kept on ice. The working solutions were obtained by diluting the 100 mM stock solution in CFFR immediately before use. GABA (Sigma) was prepared as a 100 mM stock solution in water. Dithiothreitol (DTT) (Sigma) was dissolved in water to obtain a 1 M stock solution and diluted into CFFR before each experiment.

GABA and 6a Concentration−Response Relationships. The GABA EC$_{50}$s for wt or mutant $\alpha_1\beta_2$ receptors were determined using the two-electrode voltage clamp technique on *Xenopus laevis* oocytes. To determine the GABA concentration−response relationship, progressively increasing GABA concentrations were applied to oocytes expressing wt or mutant receptors. The currents were normalized to the maximal GABA-induced current (I_{max}). The GABA concentration−response relationship was determined for each mutant by least-squares minimization (GraphPad Prism 3.0, GraphPad Software Inc., San Diego, CA; SigmaPlot 2000, SPSS Inc., Chicago, IL) of the currents to a logistic equation of the form:

$$I/I_{max} = 1/(1 + (EC_{50}/[GABA])^n)$$

where n is the Hill coefficient and EC$_{50}$ is the GABA concentration that gives rise to 50% of the maximal current. Parameters from several oocytes were averaged to obtain the mean EC$_{50}$ and Hill coefficient. Data are presented as mean ± SEM except where the number of experiments performed is two, in which case average errors are given.

For $\alpha_1\beta_2$ wt, α_1F64Cβ_2, and α_1S68Cβ_2 receptors, we also performed concentration−response experiments with **6a**, which directly activates at high concentrations, to measure the EC$_{50}$ for this compound. For **6a** dose−response curves, only two trials were performed for some mutants due to the limited supply of **6a**.

Determination of 6a IC$_{50}$. The IC$_{50}$ for **6a** was determined by coapplying progressively increasing test concentrations of **6a** with a constant GABA concentration. For each receptor, the GABA EC$_{20}$ concentration was used. We used a low GABA concentration for our inhibition experiments because of the limited availability of

6a. Inhibition was calculated as $I_{GABA+6a}/I_{GABA}$. Data were fit to the following equation:

$$\text{inhibition} = 1 - 1/(1 + (IC_{50}/[6a])^n)$$

where IC$_{50}$ is the concentration of **6a** that blocks half of I_{GABA}; [**6a**] is the concentration of **6a**, and n is the Hill coefficient.

Picrotoxinin Blockade of 6a-Induced Currents. We applied several **6a** (10 mM) test-pulses to $\alpha_1\beta_2$ receptors and recorded the induced currents. Following wash-out, we applied the open-channel blocker picrotoxinin (100 μM), immediately followed by a coapplication of **6a** and picrotoxinin (10 mM and 100 μM) and recorded the current trace.

Determination of MTS Reagent Reaction Rates. The MTS reagent was applied repeatedly in the extracellular bath for brief periods. Before and between each application of MTS reagent, the GABA-induced current was determined. For each mutant, the MTS-reagent concentration to be used was chosen based on preliminary experiments so that the reaction would proceed to completion in 1−2 min of cumulative MTS-reagent application time (MTSES$^-$ concentrations used: α_1F64C, 10 μM; α_1R66C, 250 and 500 μM; α_1S68C, 150 μM; α_1T129C, 10 nM; MTSEA-biotin concentration used: α_1R66C, 10 or 40 μM; α_1T129C, 10 nM). The peak GABA test currents were normalized to the initial GABA current, plotted as a function of the cumulative MTS-reagent application time and fitted with a monoexponential function of the form,

$$I = (I_0 - I_\infty) e^{-t\tau'} + I_\infty$$

where I_0 is the value of the GABA-induced current amplitude before modification, I_∞ is the current amplitude at the end of the reaction, t is the cumulative MTS-reagent application time, and τ' is the pseudo-first-order rate constant (s^{-1}). The second-order rate constants, τ, were calculated by dividing the pseudo-first-order time constants τ' by the MTS-reagent concentration. The second-order rate constants were independent of the MTS-reagent concentrations used. MTS-reagent reaction rates were determined for α_1F64C, α_1R66C, as well as α_1S68C containing $\alpha_1\beta_2$ GABA$_A$ receptors. Data are presented as mean ± SEM These rates were used to calculate the concentration and time of application of MTS-reagent that produces submaximal, nonsaturating inhibition.

Determination of 6a Reaction Rates in α_1R66Cβ_2 Receptors. **6a** was applied repeatedly in the extracellular bath for brief periods. Before and between each **6a** application, the GABA-induced current was determined. The **6a** reaction rate with the engineered α_1R66C was determined as described above for MTS-reagents. Once the alternating **6a** and GABA applications produced a reduced but stable GABA current, we applied a saturating amount of MTSES$^-$ (10 mM, 12 s) in order to determine whether all of the engineered cysteines had reacted with **6a**. To demonstrate that the **6a** inhibition of α_1R66C was due to formation of a disulfide bond between **6a** and the engineered cysteine thiol, we applied DTT (10 mM, 20 s) and measured the GABA current again.

Protection Assay with 6a or GABA in Mutant $\alpha_1\beta_2$ Receptors. To demonstrate that **6a** or GABA bound in close proximity to an engineered cysteine, we assayed the ability of these agonists to protect the cysteine from reaction with an MTS reagent. To maximize our ability to detect protection, we used concentrations of MTS reagents and durations of application that caused large but submaximal inhibition of the subsequent GABA test currents. For a 12 s application, the MTSES$^-$ concentrations used were: α_1F64C, 10 μM; α_1R66C, 2 mM; α_1S68C, 450 μM; and MTSEA-biotin concentration: α_1R66C, 30 μM. To detect protection for a given mutant, an initial GABA test current was determined. We coapplied a concentration-duration of MTS-reagent that produced submaximal inhibition together with **6a** (10 or 30 mM) or GABA EC$_{90}$ concentrations. After washout, the remaining GABA-induced current was determined. To determine the percent inhibition caused by the MTS + **6a** or GABA coapplication, it was important to determine the maximum extent of inhibition for each oocyte. This was determined by a subsequent application of a saturating amount of MTS reagent (MTSES$^-$ concentration: α_1F64C, 20 μM, 50 s;

α_1R66C, 10 mM, 12 s; α_1S68C, 5 mM, 12 s; MTSEA-biotin concentration: α_1R66C, 300 μM, 12 s) followed by a determination of the current induced by a subsequent GABA-test pulse. If the extent of inhibition resulting from coapplication of the MTS reagent with **6a** or GABA was less than the extent of inhibition when just the MTS reagent was applied, then we inferred that **6a** and/or GABA had protected the cysteine from modification by the MTS reagent.

The amount of reaction was calculated using the equation:

$$\%\text{reduction} = (I_0 - I)/(I_0 - I_\infty) \times 100$$

where I_0 is the value of the GABA-induced current amplitude before modification, I is the current amplitude after application of the concentration and duration of MTS-reagent that produced submaximal inhibition with or without ligand (GABA or **6a**), and I_∞ is the current amplitude at the end of the reaction after maximal inhibition. Note that the MTS-reagent rates of reaction were done by applying the reagents via a continuous perfusion system. In the protection assay, we used a syringe application system that allowed us to use small volumes because of the limited availability of **6a**.

Homology Modeling. The extracellular domains of rat GABA$_A$ receptor α_1 and β_2 subunits were modeled on the basis of the 2.2 Å crystal structure of the homologous homopentameric acetylcholine-binding protein (AChBP) with nicotine bound (PDB 1UW6). Using Deep View/Swiss Pdb-Viewer v3.7,[71] we aligned the α_1 and β_2 subunit sequences with the AChBP A and E chain, respectively.[57] The AChBP structure aligned with the raw sequence was submitted as a modeling request in Swiss model. The resulting homology modeled $\alpha_1\beta_2$ structure was subsequently subjected to energy minimization and later rendered with POV-Ray v3.6 (http://www.povray.org/).[72]

Note Added after ASAP Publication. This paper was released ASAP on July 24, 2008 with an error in an author name and in Table 5. The correct version was posted on August 7, 2008.

Supporting Information Available: Synthesis descriptions for compounds **1a**−**g**, **2a**−**g**, **3a**−**g**, **4a**−**g**, **7a,b**, **8a**−**e**, **12a,d**, **13a,d**, **14a**, **15a**, and **18**, together with spectroscopic data. IR-Data for all compounds and elemental analysis data applied to target compounds. This material is available free of charge via the Internet at http://pubs.acs.org.

References

(1) Barnard, E. A.; Skolnick, P.; Olsen, R. W.; Mohler, H.; Sieghart, W.; Biggio, G.; Braestrup, C.; Bateson, A. N.; Langer, S. Z. International Union of Pharmacology. XV. Subtypes of gamma-aminobutyric acidA receptors: classification on the basis of subunit structure and receptor function. *Pharmacol. Rev.* **1998**, *50*, 291–313.

(2) Bonnert, T. P.; McKernan, R. M.; Farrar, S.; le Bourdelles, B.; Heavens, R. P.; Smith, D. W.; Hewson, L.; Rigby, M. R.; Sirinathsinghji, D. J.; Brown, N.; Wafford, K. A.; Whiting, P. J. Theta, a novel gamma-aminobutyric acid type A receptor subunit. *Proc. Natl. Acad. Sci. U.S.A.* **1999**, *96*, 9891–9896.

(3) Sinkkonen, S. T.; Hanna, M. C.; Kirkness, E. F.; Korpi, E. R. GABA(A) receptor epsilon and theta subunits display unusual structural variation between species and are enriched in the rat locus ceruleus. *J. Neurosci.* **2000**, *20*, 3588–3595.

(4) Böhme, I.; Rabe, H.; Lüddens, H. Four amino acids in the alpha subunits determine the gamma-aminobutyric acid sensitivities of GABAA receptor subtypes. *J. Biol. Chem.* **2004**, *279*, 35193–35200.

(5) Sieghart, W.; Sperk, G. Subunit composition, distribution and function of GABA(A) receptor subtypes. *Curr. Top. Med. Chem.* **2002**, *2*, 795–816.

(6) Nusser, Z.; Sieghart, W.; Somogyi, P. Segregation of different GABA$_A$ receptors to synaptic and extrasynaptic membranes of cerebellar granule cells. *J. Neurosci.* **1998**, *18*, 1693–1703.

(7) Fritschy, J. M.; Johnson, D. K.; Mohler, H.; Rudolph, U. Independent assembly and subcellular targeting of GABA(A)-receptor subtypes demonstrated in mouse hippocampal and olfactory neurons in vivo. *Neurosci. Lett.* **1998**, *249*, 99–102.

(8) Luddens, H.; Korpi, E. R. Biological function of GABAA/benzodiazepine receptor heterogeneity. *J. Psychiatr. Res.* **1995**, *29*, 77–94.

(9) Quirk, K.; Blurton, P.; Fletcher, S.; Leeson, P.; Tang, F.; Mellilo, D.; Ragan, C. I.; McKernan, R. M. [3H]L-655,708, a novel ligand selective for the benzodiazepine site of GABAA receptors which contain the alpha 5 subunit. *Neuropharmacology* **1996**, *35*, 1331–1335.

(10) Skolnick, P.; Hu, R. J.; Cook, C. M.; Hurt, S. D.; Trometer, J. D.; Liu, R.; Huang, Q.; Cook, J. M. [3H]RY 80: A high-affinity, selective ligand for gamma-aminobutyric acidA receptors containing alpha-5 subunits. *J. Pharmacol. Exp. Ther.* **1997**, *283*, 488–493.

(11) Luddens, H.; Pritchett, D. B.; Kohler, M.; Killisch, I.; Keinanen, K.; Monyer, H.; Sprengel, R.; Seeburg, P. H. Cerebellar GABAA receptor selective for a behavioural alcohol antagonist. *Nature* **1990**, *346*, 648–651.

(12) Wisden, W.; Seeburg, P. H. GABA$_A$ receptor channels: from subunits to functional entities. *Curr. Opin. Neurobiol.* **1992**, *2*, 263–269.

(13) Pritchett, D. B.; Sontheimer, H.; Shivers, B. D.; Ymer, S.; Kettenmann, H.; Schofield, P. R.; Seeburg, P. H. Importance of a novel GABA$_A$ receptor subunit for benzodiazepine pharmacology. *Nature* **1989**, *338*, 582–585.

(14) Sigel, E.; Buhr, A. The benzodiazepine binding site of GABA$_A$ receptors. *Trends Pharmacol. Sci.* **1997**, *18*, 425–429.

(15) Saarelainen, K. S.; Ranna, M.; Rabe, H.; Sinkkonen, S. T.; Moykkynen, T.; Uusi-Oukari, M.; Linden, A. M.; Luddens, H.; Korpi, E. R. Enhanced behavioral sensitivity to the competitive GABA agonist, gaboxadol, in transgenic mice over-expressing hippocampal extrasynaptic alpha6beta GABA(A) receptors. *J. Neurochem.* **2008**, *105*, 338–350.

(16) Korpi, E. R.; Luddens, H. Furosemide interactions with brain GABAA receptors. *Br. J. Pharmacol.* **1997**, *120*, 741–748.

(17) Korpi, E. R.; Kuner, T.; Seeburg, P. H.; Luddens, H. Selective antagonist for the cerebellar granule cell-specific gamma- aminobutyric acid type A receptor. *Mol. Pharmacol.* **1995**, *47*, 283–289.

(18) Korpi, E. R.; Wong, G.; Luddens, H. Subtype specificity of gamma-aminobutyric acid type A receptor antagonism by clozapine. *Naunyn—Schmiedebergs Arch. Pharmacol.* **1995**, *352*, 365–373.

(19) Barbee, J. G. Memory, benzodiazepines, and anxiety: integration of theoretical and clinical perspectives. *J. Clin. Psychiatry* **1993**, *54 Suppl*, 86–97, discussion 98−101.

(20) Salinas, J. A.; McGaugh, J. L. Muscimol induces retrograde amnesia for changes in reward magnitude. *Neurobiol. Learn. Mem.* **1995**, *63*, 277–285.

(21) Huang, Q.; Liu, R.; Zhang, P.; He, X.; McKernan, R.; Gan, T.; Bennett, D. W.; Cook, J. M. Predictive models for GABAA/benzodiazepine receptor subtypes: studies of quantitative structure−activity relationships for imidazobenzodiazepines at five recombinant GABAA/benzodiazepine receptor subtypes [alphaxbeta3gamma2 ($x = 1−3$, 5, and 6)] via comparative molecular field analysis. *J. Med. Chem.* **1998**, *41*, 4130–42.

(22) Huang, Q.; He, X.; Ma, C.; Liu, R.; Yu, S.; Dayer, C. A.; Wenger, G. R.; McKernan, R.; Cook, J. M. Pharmacophore/receptor models for GABA(A)/BzR subtypes (alpha1beta3gamma2, alpha5beta3gamma2, and alpha6beta3gamma2) via a comprehensive ligand-mapping approach. *J. Med. Chem.* **2000**, *43*, 71–95.

(23) Li, X.; Cao, H.; Zhang, C.; Furtmueller, R.; Fuchs, K.; Huck, S.; Sieghart, W.; Deschamps, J.; Cook, J. M. Synthesis, in vitro affinity, and efficacy of a bis-8-ethynyl-4H-imidazo[1,5a]-[1,4]benzodiazepine analogue, the first bivalent alpha5 subtype selective BzR/GABA(A) antagonist. *J. Med. Chem.* **2003**, *46*, 5567–5570.

(24) Cook, J. B.; Foster, K. L.; Eiler, W. J., II; McKay, P. F.; Woods, J., II; Harvey, S. C.; Garcia, M.; Grey, C.; McCane, S.; Mason, D.; Cummings, R.; Li, X.; Cook, J. M.; June, H. L. Selective GABAA alpha5 benzodiazepine inverse agonist antagonizes the neurobehav-

ioral actions of alcohol. *Alcohol.: Clin. Exp. Res.* **2005**, *29*, 1390–401.

(25) Albaugh, P. A.; Marshall, L.; Gregory, J.; White, G.; Hutchison, A.; Ross, P. C.; Gallagher, D. W.; Tallman, J. F.; Crago, M.; Cassella, J. V. Synthesis and biological evaluation of 7,8,9,10-tetrahydroimidazo[1,2-*c*]pyrido[3,4-*e*]pyrimdin-5(6*H*)-ones as functionally selective ligands of the benzodiazepine receptor site on the GABA(A) receptor. *J. Med. Chem.* **2002**, *45*, 5043–5051.

(26) Collins, I.; Moyes, C.; Davey, W. B.; Rowley, M.; Bromidge, F. A.; Quirk, K.; Atack, J. R.; McKernan, R. M.; Thompson, S. A.; Wafford, K.; Dawson, G. R.; Pike, A.; Sohal, B.; Tsou, N. N.; Ball, R. G.; Castro, J. L. 3-Heteroaryl-2-pyridones: benzodiazepine site ligands with functional delectivity for alpha 2/alpha 3-subtypes of human GABA(A) receptor-ion channels. *J. Med. Chem.* **2002**, *45*, 1887–1900.

(27) Mitchinson, A.; Atack, J. R.; Blurton, P.; Carling, R. W.; Castro, J. L.; Curley, K. S.; Russell, M. G.; Marshall, G.; McKernan, R. M.; Moore, K. W.; Narquizian, R.; Smith, A.; Street, L. J.; Thompson, S. A.; Wafford, K. 2,5-Dihydropyrazolo[4,3-*c*]pyridin-3-ones: functionally selective benzodiazepine binding site ligands on the GABAA receptor. *Bioorg. Med. Chem. Lett.* **2004**, *14*, 3441–4.

(28) Yasumatsu, H.; Morimoto, Y.; Yamamoto, Y.; Takehara, S.; Fukuda, T.; Nakao, T.; Setoguchi, M. The pharmacological properties of Y-23684, a benzodiazepine receptor partial agonist. *Br. J. Pharmacol.* **1994**, *111*, 1170–8.

(29) Haefely, W.; Martin, J. R.; Schoch, P. Novel anxiolytics that act as partial agonists at benzodiazepine receptors. *Trends Pharmacol. Sci.* **1990**, *11*, 452–6.

(30) Grunwald, C.; Rundfeldt, C.; Lankau, H. J.; Arnold, T.; Hofgen, N.; Dost, R.; Egerland, U.; Hofmann, H. J.; Unverferth, K. Synthesis, pharmacology, and structure−activity relationships of novel imidazolones and pyrrolones as modulators of GABAA receptors. *J. Med. Chem.* **2006**, *49*, 1855–1866.

(31) Krogsgaard-Larsen, P.; Frolund, B.; Jorgensen, F. S.; Schousboe, A. GABAA receptor agonists, partial agonists, and antagonists. Design and therapeutic prospects. *J. Med. Chem.* **1994**, *37*, 2489–2505.

(32) Rabe, H.; Picard, R.; Uusi-Oukari, M.; Hevers, W.; Lüddens, H.; Korpi, E. R. Coupling between agonist and chloride ionophore sites of the GABA(A) receptor: agonist/antagonist efficacy of 4-PIOL. *Eur. J. Pharmacol.* **2000**, *409*, 233–242.

(33) Byberg, J. R.; Labouta, I. M.; Falch, E.; Hjeds, H.; Krogsgaard-Larsen, P.; Curtis, D. R.; Gynther, B. D. Synthesis and biological activity of a GABAA agonist which has no effect on benzodiazepine binding and of structurally related glycine antagonists. *Drug Des. Delivery* **1987**, *1*, 261–274.

(34) Frolund, B.; Jensen, L. S.; Storustovu, S. I.; Stensbol, T. B.; Ebert, B.; Kehler, J.; Krogsgaard-Larsen, P.; Liljefors, T. 4-Aryl-5-(4-piperidyl)-3-isoxazolol GABAA antagonists: synthesis, pharmacology, and structure-activity relationships. *J. Med. Chem.* **2007**, *50*, 1988–1992.

(35) Krehan, D.; Storustovu, S. I.; Liljefors, T.; Ebert, B.; Nielsen, B.; Krogsgaard-Larsen, P.; Frolund, B. Potent 4-arylalkyl-substituted 3-isothiazolol GABA(A) competitive/noncompetitive antagonists: synthesis and pharmacology. *J. Med. Chem.* **2006**, *49*, 1388–1396.

(36) Frolund, B.; Jensen, L. S.; Guandalini, L.; Canillo, C.; Vestergaard, H. T.; Kristiansen, U.; Nielsen, B.; Stensbol, T. B.; Madsen, C.; Krogsgaard-Larsen, P.; Liljefors, T. Potent 4-aryl- or 4-arylalkyl-substituted 3-isoxazolol GABA(A) antagonists: synthesis, pharmacology, and molecular modeling. *J. Med. Chem.* **2005**, *48*, 427–439.

(37) Frolund, B.; Tagmose, L.; Jorgensen, A. T.; Kristiansen, U.; Stensbol, T. B.; Liljefors, T.; Krogsgaard-Larsen, P. Design and synthesis of a new series of 4-alkylated 3-isoxazolol GABA A antagonists. *Eur. J. Med. Chem.* **2003**, *38*, 447–449.

(38) Mortensen, M.; Frolund, B.; Jorgensen, A. T.; Liljefors, T.; Krogsgaard-Larsen, P.; Ebert, B. Activity of novel 4-PIOL analogues at human alpha 1 beta 2 gamma 2S GABA(A) receptors−correlation with hydrophobicity. *Eur. J. Pharmacol.* **2002**, *451*, 125–132.

(39) Frolund, B.; Jorgensen, A. T.; Tagmose, L.; Stensbol, T. B.; Vestergaard, H. T.; Engblom, C.; Kristiansen, U.; Sanchez, C.; Krogsgaard-Larsen, P.; Liljefors, T. Novel class of potent 4-arylalkyl substituted 3-isoxazolol GABA(A) antagonists: synthesis, pharmacology, and molecular modeling. *J. Med. Chem.* **2002**, *45*, 2454–2468.

(40) Frolund, B.; Kristiansen, U.; Brehm, L.; Hansen, A. B.; Krogsgaard-Larsen, P.; Falch, E. Partial GABAA receptor agonists. Synthesis and in vitro pharmacology of a series of nonannulated analogs of 4,5,6,7-tetrahydroisoxazolo[5,4-*c*]pyridin-3-ol. *J. Med. Chem.* **1995**, *38*, 3287–3296.

(41) Akabas, M. H.; Stauffer, D. A.; Xu, M.; Karlin, A. Acetylcholine receptor channel structure probed in cysteine-substitution mutants. *Science* **1992**, *258*, 307–310.

(42) Sigel, E.; Baur, R.; Kellenberger, S.; Malherbe, P. Point mutations affecting antagonist affinity and agonist dependent gating of GABAA receptor channels. *EMBO J.* **1992**, *11*, 2017–2023.

(43) Hartvig, L.; Lukensmejer, B.; Liljefors, T.; Dekermendjian, K. Two conserved arginines in the extracellular N-terminal domain of the GABA(A) receptor alpha(5) subunit are crucial for receptor function. *J. Neurochem.* **2000**, *75*, 1746–1753.

(44) Westh-Hansen, S. E.; Witt, M. R.; Dekermendjian, K.; Liljefors, T.; Rasmussen, P. B.; Nielsen, M. Arginine residue 120 of the human GABAA receptor alpha 1, subunit is essential for GABA binding and chloride ion current gating. *Neuroreport* **1999**, *10*, 2417–2421.

(45) Smith, G. B.; Olsen, R. W. Identification of a [³H]muscimol photo-affinity substrate in the bovine gamma-aminobutyric acidA receptor alpha subunit. *J. Biol. Chem.* **1994**, *269*, 20380–20387.

(46) Holden, J. H.; Czajkowski, C. Different residues in the GABAA receptor alpha 1T60-alpha 1K70 region mediate GABA and SR-95531 actions. *J. Biol. Chem.* **2002**, *277*, 18785–18792.

(47) Boileau, A. J.; Evers, A. R.; Davis, A. F.; Czajkowski, C. Mapping the agonist binding site of the GABAA receptor: evidence for a beta-strand. *J. Neurosci.* **1999**, *19*, 4847–4854.

(48) Kloda, J. H.; Czajkowski, C. Agonist-, antagonist-, and benzodiazepine-induced structural changes in the alpha1 Met113-Leu132 region of the GABAA receptor. *Mol. Pharmacol.* **2007**, *71*, 483–493.

(49) Celie, P. H.; van Rossum-Fikkert, S. E.; van Dijk, W. J.; Brejc, K.; Smit, A. B.; Sixma, T. K. Nicotine and carbamylcholine binding to nicotinic acetylcholine receptors as studied in AChBP crystal structures. *Neuron* **2004**, *41*, 907–914.

(50) Aranda, G.; Dessolin, M.; Golfier, M.; Guillerez, M. G. ¹³C NMR Study of some Derivatives of 1,3,4-Oxadiazoles, 1,3,4-Thiadiazoles and Isosydnones. *Org. Magn. Res.* **1982**, *18*, 159–164.

(51) Roberts, D. D.; Lewis, S. D.; Ballou, D. P.; Olson, S. T.; Shafer, J. A. Reactivity of small thiolate anions and cysteine-25 in papain towards methylmethanethiosulfonate. *Biochemistry* **1986**, *25*, 5595–5601.

(52) Horenstein, J.; Akabas, M. H. Location of a high affinity Zn²⁺ binding site in the channel of alpha1beta1 gamma-aminobutyric acid A receptors. *Mol. Pharmacol.* **1998**, *53*, 870–877.

(53) Baumann, S. W.; Baur, R.; Sigel, E. Subunit arrangement of gamma-aminobutyric acid type A receptors. *J. Biol. Chem.* **2001**, *276*, 36275–36280.

(54) Frolund, B.; Tagmose, L.; Liljefors, T.; Stensbol, T. B.; Engblom, C.; Kristiansen, U.; Krogsgaard-Larsen, P. A novel class of potent 3-isoxazolol GABA(A) antagonists: design, synthesis, and pharmacology. *J. Med. Chem.* **2000**, *43*, 4930–4833.

(55) Krogsgaard-Larsen, P.; Mikkelsen, H.; Jacobsen, P.; Falch, E.; Curtis, D. R.; Peet, M. J.; Leah, J. D. 4,5,6,7-Tetrahydroisothiazolo[5,4-*c*]pyridin-3-ol and related analogues of THIP. Synthesis and biological activity. *J. Med. Chem.* **1983**, *26*, 895–900.

(56) Brejc, K.; van Dijk, W. J.; Smit, A. B.; Sixma, T. K. The 2.7 A structure of AChBP, homologue of the ligand-binding domain of the nicotinic acetylcholine receptor. *Novartis Found. Symp.* **2002**, *245*, 22–29, discussion 29−32, 165−168.

(57) Cromer, B. A.; Morton, C. J.; Parker, M. W. Anxiety over GABA(A) receptor structure relieved by AChBP. *Trends Biochem. Sci.* **2002**, *27*, 280–7.

(58) Brejc, K.; van Dijk, W. J.; Klaassen, R. V.; Schuurmans, M.; van Der Oost, J.; Smit, A. B.; Sixma, T. K. Crystal structure of an ACh-binding protein reveals the ligand-binding domain of nicotinic receptors. *Nature* **2001**, *411*, 269–276.

(59) Wagner, D. A.; Czajkowski, C. Structure and dynamics of the GABA binding pocket: A narrowing cleft that constricts during activation. *J. Neurosci.* **2001**, *21*, 67–74.

(60) Jin, R.; Banke, T. G.; Mayer, M. L.; Traynelis, S. F.; Gouaux, E. Structural basis for partial agonist action at ionotropic glutamate receptors. *Nat. Neurosci.* **2003**, *6*, 803–810.

(61) Aboul-Enein, M. N.; Azzouny, A. A.; Abdallah, N. A.; El-Shabrawy Makhlouf, A. A.; Werner, W. Synthesis of Certain 5-Piperidyl-1,3,4-Oxadiazol-2(3*H*)-ones and -2(3*H*)-thiones having Nonulcerogenic, Antiinflammatory and Analgesic Activities. *Sci. Pharm.* **1995**, *63*, 175–190.

(62) Bentley, K. W.; Burton, M.; Uff, B. C. 1,3,4-Oxadiazol-2(3*H*)-one Formation from *N*-Acylaminobiurets and Related Compounds and from *S*-Benzyl 3-Acyl(thiocarbazates). *J. Chem. Soc., Perkin Trans. 1* **1982**, *9*, 2019–2021.

(63) Dornow, A.; K., B. Notiz über die Darstellung von 1.3.4-Oxadiazolon-(5) und seinen C2-alkylierten Derivaten. *Chem. Ber.* **1949**, *82*, 121–123.

(64) Hoggarth, E. 2-Benzoyldithiocarbazinic Acid and Related Compounds. *J. Chem. Soc., Perkin Trans. 1* **1952**, 4811–4817.

(65) Horning, D. E.; Muchowski, J. M. Five-membered Heterocyclic Thiones Part I. 1,3,4-Oxadiazol-2-thione. *Can. J. Chem.* **1972**, *50*, 3079–3083.

(66) Korpi, E. R.; Luddens, H. Regional gamma-aminobutyric acid sensitivity of t- butylbicyclophosphoro[35S]thionate binding depends on gamma-aminobutyric acidA receptor alpha subunit. *Mol. Pharmacol.* **1993**, *44*, 87–92.

(67) Luddens, H.; Korpi, E. R. GABA antagonists differentiate between recombinant GABAA/benzodiazepine receptor subtypes. *J. Neurosci.* **1995**, *15*, 6957–6962.

(68) Pritchett, D. B.; Seeburg, P. H. Gamma-aminobutyric acidA receptor alpha 5-subunit creates novel type II benzodiazepine receptor pharmacology. *J. Neurochem.* **1990**, *54*, 1802–1804.

(69) Hamill, O. P.; Marty, A.; Neher, E.; Sakmann, B.; Sigworth, F. J. Improved patch-clamp techniques for high-resolution current recording from cells and cell-free membrane patches. *Pflugers Arch.* **1981**, *391*, 85–100.

(70) Horenstein, J.; Wagner, D. A.; Czajkowski, C.; Akabas, M. H. Protein mobility and GABA-induced conformational changes in GABA$_A$ receptor pore-lining M2 segment. *Nat. Neurosci.* **2001**, *4*, 477–485.

(71) Schwede, T.; Kopp, J.; Guex, N.; Peitsch, M. C. SWISS-MODEL: An automated protein homology-modeling server. *Nucleic Acids Res.* **2003**, *31*, 3381–3385.

(72) Bali, M.; Akabas, M. H. Defining the propofol binding site location on the GABAA receptor. *Mol. Pharmacol.* **2004**, *65*, 68–76.